Chemistry–A European Journal

Supporting Information

An Assay for Screening Potential Drug Candidates for Alzheimer's Disease That Act as Chaperones of the Transthyretin and Amyloid-β Peptides Interaction

Ellen Y. Cotrina,[a] Ana Gimeno,[c, d, e] Jordi Llop,[b] Jesús Jiménez-Barbero,[c, d, e] Jordi Quintana,[f] Rafel Prohens,[g] Isabel Cardoso,[h] and Gemma Arsequell*[a]

Table of contents

Abbreviations

AD, Alzheimer's disease; Aβ, amyloid beta; BSA, Bovine Serum Albumin; DCPA, *N*-(3,5-dichlorophenyl)anthranilic; DFPA, *N*-(3,5-difluorophenyl)anthranilic; DIF, diflunisal; DMSO, dimethyl sulfoxide; DoE, Design of Experiments; HEPES, *N*-(2-hydroxyethyl) piperazine-N′-(2-ethanesulfonic acid); IDIF, iododiflunisal; HTS, High-Throughput Screening; IPTG, Isopropyl β-D-1-thiogalactopyranoside; ITC, Isothermal Titration Calorimetry; MALDI-ToF MS, Matrix-assisted Laser Desorption/Ionization Time-of-Flight Mass Spectrometry; MW- SPPS, Microwave Solid-Phase Peptide Synthesis; NSAID, Non-Steroidal Anti-Inflammatory Drug; RA, reduction of aggregates; RP-HPLC, Reversed Phase High-Performance Liquid Chromatography; SDS-PAGE, Sodium Dodecyl Sulfate Polyacrylamide Gel Electrophoresis; SMCs, small-molecule chaperones; SPPS; Solid-Phase Peptide Synthesis; STD-NMR, Saturation Transfer Difference Nuclear Magnetic Resonance; TEM, Transmission Electron Microscopy TFA, Trifluoroacetic acid; TIS; *Tris*-isopropylsilane; Tris, Tris(hydroxymethyl)-aminomethane; UPLC-ToF MS, ultra-high performance liquid chromatography Time-of-Flight Mass Spectrometry; and wtTTR, wild-type transthyretin.

Hard lessons from Alzheimer's Disease (AD) drug discovery

The number of people affected by Alzheimer's Disease (AD) are estimated to be a staggering 14 million in the USA alone, and 100 million worldwide by 2050.[1] Accordingly, there is an urgent need to discover and develop new therapeutic drugs to prevent, delay the onset, halt the progression, or improve the symptoms of AD.[2] Regrettably, research focused on the development of AD therapies is having a very poor success rate.[3,4] Up to now, only 5 drugs are approved for treatments of the symptoms of AD. No new drugs have been approved since 2003 and there are no approved disease-modifying drugs for AD.[5] As a comparison, the success rate for the development of oncological compounds is approximately 19%, which drives pharma companies to invest mainly in areas other than AD. In addition, failures of drugs that created high expectation, such as Verubecestat (MK-8931).[6-8] Semagacestat, (mAb) Bapineuzumab[9] and the passive immunity drug Solanezumab (Eli Lilly)[10] that reached phase III, are even casting doubts about the validity of the amyloid hypothesis[11] of AD and driving big pharma such as Pfizer to withdraw from dementia research.[12-13]

Many explanations for the very low rate of success of drug development for AD have been proposed. Lack of predictive validity of animal models, inadequate or incomplete understanding of the biology of AD, slowness in recruitment for trials and heterogeneity of patients, testing single therapies where combinations may be compulsory, wrong treatment target, incorrect drug doses, test therapies applied in too advanced disease stages, lack of reliable biomarkers for the myriad affected biochemical processes, wrong choice of clinical endpoints, lack of efficacy of experimental therapies, appearance of unacceptable side effects, lack of new chemical entities (NCEs) resulting in few candidates entering Phase I, may be valid reasons.[5, 14-17]

New approaches are clearly needed in to overcome this high rate of attrition of compounds for AD. Possibilities include the development of hypotheses derived from better disease knowledge, candidate lead compounds, repurposed drugs, immunotherapy, physical interventions and/or improved clinical trials. Thus, with the aim to contribute new candidate drugs that, after preclinical tests, may feed the currently exhausted pipeline of drugs in phase I for AD, here we describe a methodological approach to screen for novel and existing chemical entities that may stabilize Aβ peptides in solution and facilitate their clearance from brain.

References:

1. Alzheimer's Association Report 2019 Alzheimer's disease facts and figures Alzheimer's Association. *Alzheimers Dement.* **2019**, 15, 321-387.
2. S. O. Bachurin, E. V. Bovina, A. A. Ustyugov, Drugs in Clinical Trials for Alzheimer's Disease: The Major Trends. *Med. Res. Rev.* **2017**, *37*, 1186-1225.
3. Doig, A. J.; Del Castillo-Frias M. P.; Berthoumieu, O.; Tarus, B.; Nasica-Labouze, J.; Sterpone, F.; Nguyen P. H.; Hooper, N. M.; Faller, P.; Derreumaux, P. Why Is Research on Amyloid-β Failing to Give New Drugs for Alzheimer's Disease? *ACS Chem. Neurosci.,* **2017***, 8*, 1435-1437.
4. D. Mehta, R. Jackson, G. Paul, J. Shi, M. Sabbagh, Why do trials for Alzheimer's disease drugs keep failing? A discontinued drug perspective for 2010-2015. *Expert Opin. Investig. Drugs.* **2017**, *26*, 735-739.
5. J. Cummings, G. Lee, A. Ritter, M. Sabbagh, K. Zhong, Alzheimer's disease drug development pipeline: 2019. *Alzheimers Dement* (N Y). **2019**, *5*, 272-293.
6. N. Hawkes, Merck ends trial of potential Alzheimer's drug verubecestat. *BMJ.*, 2017, 356:j845.
7. A. Mullard, A. BACE inhibitor bust in Alzheimer trial. *Nat. Rev. Drug Discov.* **2017**, *16*, 155.
8. M. F. Egan, J. M. Kost, T. Voss, Y. Mukai, P. S. Aisen, J. L. Cummings, P. N. Tariot, B. Vellas, C. H. van Dyck, M. Boada, Y. Zhang, W. Li, C. Furtek, E. Mahoney, L. Harper Mozley, Y. Mo, C. Sur, D. Michelson, Randomized Trial of Verubecestat for Prodromal Alzheimer's Disease. *N. Engl. J. Med.* **2019**, *380*, 1408-1420.
9. M. Gold, Phase II clinical trials of anti-amyloid β antibodies: When is enough, enough? *Alzheimers Dement (N Y).* **2017**, *3*, 402-409.

10. C. A. Sacks, J. Avorn, A. S. Kesselheim, The Failure of Solanezumab - How the FDA Saved Taxpayers Billions. *N. Engl. J. Med.* **2017**, *376*, 1706-1708.
11. F. Kametani, M. Hasegawa, Reconsideration of Amyloid Hypothesis and Tau Hypothesis in Alzheimer's Disease. *Front. Neurosci.* **2018**, *12*, 25.
12. F. Prati, G. Bottegoni, M. L. Bolognesi, A. Cavalli, BACE-1 Inhibitors: From Recent Single-Target Molecules to Multitarget Compounds for Alzheimer's Disease. *J. Med. Chem.* **2018**, *61*, 619-637.
13. G. Watts, Prospects for dementia research. *Lancet* **2018**, *391*, 416.
14. J. Cummings, Lessons Learned from Alzheimer Disease: Clinical Trials with Negative Outcomes. *Clin. Transl. Sci.* **2018**, *11*, 147-152.
15. J. Cummings, A. Ritter, K. Zhong, Clinical Trials for Disease-Modifying Therapies in Alzheimer's Disease: A Primer, Lessons Learned, and a Blueprint for the Future. *J. Alzheimers Dis.* **2018**, *64* (s1): S3-S22.
16. J. Cummings, H. H. Feldman, P. Scheltens, The "rights" of precision drug development for Alzheimer's disease. *Alz. Res.Ther*., **2019**, *11*, 76.
17. J. L. Molinuevo, C. Minguillon, L. Rami, J. D. Gispert, The Rationale Behind the New Alzheimer's Disease Conceptualization: Lessons Learned During the Last Decades. *J. Alzheimers Dis.* **2018**, *62*, 1067-1077.

Comparison to other assays to study Aβ self-assembly process in the presence of other chaperone or non-chaperone proteins. Advantages of our assay.

Several methods, either tracking the amyloid associated toxicity in cell lines or the amyloid aggregation *in vitro*, are used to screen anti-Alzheimer anti-amyloid drugs. Only some of them have been extrapolated to study the Aβ self-assembly process in the presence of chaperone or non-chaperone proteins. Some examples reported in the literature to study binary protein-protein interactions, are:

a) Fluorescence Anisotropy to study the interaction between the retinol-binding protein and TTR,[1]
b) Surface Plasmon Resonance (SPR) studies using Aβ as a ligand immobilized in the chips surface,[2]
c) Electrochemical strategies to study the interaction between Aβ peptides and gelsolin.[3, 4]
d) Thioflavin-T fluorescence assays to study BSA/Aβ interactions[5] and, more recently, the interaction between protein tau and Aβ,[6]

Of these described procedures, only a scarce minority have been used to explore ternary interactions. Some examples found in the literature are: a) the ThT study of a blocking peptide of the ApoE/Aβ interaction;[7,8] b) the study of the interference of the Retinol-Binding Protein (RBP) in the TTR/Aβ interaction;[9] c) the SPR study of the influence of unsaturated fatty acids on HSA/Aβ(1-40/1-42) interactions;[10] and d) the ThT study of other molecules suppressing the HSA/Aβ(1-40) interactions.[11] In contrast with SPR based methods, our assay is performed in solution and no need for Aβ immobilization is required.

Additionally, our assay has the following advantages:

a) The entire process is run in a 96-well format, minimizes sample handling and mimics physiological conditions such as temperature and pH in vitro.
b) It makes use of Aβ(12-28) which has analogous properties as Aβ(1-42), but is a less expensive more stable peptide, and makes use of recombinant TTR.
c) By UV monitoring of the turbidity for 6 h in the HTS assay, the chaperoning potency of small-molecule compounds can be determined.

d) The assay has been checked for reproducibility by statistical analysis and validated against of a small set of previously assayed good TTR ligands that behave as efficient small-molecule chaperones of the TTR−Aβ interactions.

The rapid and simple HTS assay developed in this work is robust, reproducible and provides quantitative information on the aggregation process and helps at identifying novel chaperones of the TTR−Aβ interaction. Furthermore, the assay could be of use and implemented to evaluate other Aβ-binding proteins.

References:

1. C. Folli, C. R. Favilla, R. Berni, The interaction between retinol-binding protein and transthyretin analyzed by fluorescence anisotropy. *Methods Mol. Biol.* **2010***,* 652, 189-207.
2. F. Bellia, V. Lanza, S. García-Viñuales, I. M. M. Ahmed, A. Pietropaolo, C. Iacobucci, G. Malgieri, G. D'Abrosca, R. Fattorusso, V. G. Nicoletti, D. Sbardella, G. R. Dundo, M. Coletta, L. Pirone, E. Pedone, D. Calcagno, G. Grasso, D. Milardi, Ubiquitin binds the amyloid β peptide and interferes with its clearance pathways. *Chem. Sci.* **2019**, *10*, 2732-2742.
3. Y. Yu, X: Sun, D. Tang, C. Li, L. Zhang, D. Nie, X. Yin, G. Shi, Gelsolin bound β-amyloid peptides(1-40/1-42): electrochemical evaluation of levels of soluble peptide associated with Alzheimer's disease. *Biosens. Bioelectron.* **2015**, *68*, 115-121.
4. Y. Yu, L. Zhang, C. Li, X. Sun, D. Tang, G. Shi, A method for evaluating the level of soluble β-amyloid(1-40/1-42) in Alzheimer's disease based on the binding of gelsolin to β-amyloid peptides. *Angew. Chem. Int. Ed.* **2014***, 53*, 12832-12835.
5. A. A. Reyes Barcelo, F. J. Gonzalez-Velasquez, M. A. Moss, Soluble aggregates of the amyloid-beta peptide are trapped by serum albumin to enhance amyloid-beta activation of endothelial cells. *J. Biol. Eng.* **2009**, *3*, 5.
6. C. Wallin, Y. Hiruma, S. K. T. S. Wärmländer, I. Huvent, J. Jarvet, J. P. Abrahams, A. Gräslund, G. Lippens, J. Luo, The Neuronal Tau Protein Blocks in Vitro Fibrillation of the Amyloid-β (Aβ) Peptide at the Oligomeric Stage. *J. Am. Chem. Soc.* **2018***, 140*, 8138-8146.
7. M. Sadowski, J. Pankiewicz, H. Scholtzova, J. A. Ripellino, Y. Li, S. D. Schmidt, P. M. Mathews, J. D. Fryer, D. M. Holtzman, E. M. Sigurdsson, T. Wisniewski, A synthetic peptide blocking the apolipoprotein E/beta-amyloid binding mitigates beta-amyloid toxicity and fibril formation in vitro and reduces beta-amyloid plaques in transgenic mice. *Am. J. Pathol.* **2004**, *165*, 937-948.
8. S. Liu, S. Park, G. Allington, F. Prelli, Y. Sun, M. Martá-Ariza, H. Scholtzova, G. Biswas, B. Brown, P. B. Verghese, P. D. Mehta, Y. U. Kwon, T. Wisniewski, Targeting Apolipoprotein E/Amyloid β Binding by Peptoid CPO_Aβ17-21 P Ameliorates Alzheimer's Disease Related Pathology and Cognitive Decline. *Sci. Rep*. **2017**, **7**, 8009.
9. P. Mangrolia, R. M. Murphy, Retinol-Binding Protein Interferes with Transthyretin-Mediated β-Amyloid Aggregation Inhibition. *Biochemistry* 2018, **57**, 5029-5040.
10. E. A. Litus, A. S. Kazakov, A. S. Sokolov, E. L. Nemashkalova, E. I. Galushko, U. F. Dzhus, V. V. Marchenkov, O.V. Galzitskaya, E. A. Permyakov, S. E. Permyakov, The binding of monomeric amyloid β peptide to serum albumin is affected by major plasma unsaturated fatty acids. *Biochem. Biophys. Res. Commun.* **2019**, *510*, 248-253.
11. D. C. Bode, H. F. Stanyon, T. Hirani, M. D. Baker, J. Nield, J. H. Viles, Serum Albumin's Protective Inhibition of Amyloid-β Fiber Formation Is Suppressed by Cholesterol, Fatty Acids and Warfarin. *J. Mol. Biol.* **2019**, *430*, 919-934.

The Aβ(12−28) peptide

The short Aβ amyloid peptide (VHHQKLVFFAEDVGSNK) has been extensively studied and is reported to exhibit essentially identical neurotoxic behavior and fibril formation features as the Aβ(1-42) and (1-40) peptides and thus has been used as a short model of the full Aβ peptides.[1]Structural studies of this Aβ(12-28) amyloid sequence have shown to contain a domain known as the "hydrophobic core" (residues 17-21) and a β-turn (residues 22-28).[2] These peptide stretches look essential for the formation of large aggregates and fibrils in the Aβ(1-40) and Aβ(1-42) longer peptides.[3] Thus, mutations in the hydrophobic core such as Phe19/Pro19 have a large influence on the aggregation properties and even prevent fibrillization.[4] Also, the aggregation characteristics of Aβ(12−28) have a strong pH dependence.[5] The conformational characteristics of the Aβ(12-28) amyloid peptide have been studied extensively.[6] Molecular dynamic studies[7] and investigations on the gas-phase structure of the amyloid peptide Aβ(12–28) have been published.[8]

References

[1] a) P. E. Eraser, L. Lévesque, D. R. McLachlan, Alzheimer Aβ amyloid forms an inhibitory neuronal substrate, *J. Neurochem.* **1994***, 62*, 1227-1230; b) J. F. Flood, J. E. Morley, E. Roberts, An amyloid β-protein fragment, Aβ(12-28), equipotently impairs post-training memory processing when injected into different limbic system structures, *Brain Res.* **1994**, *663*, 271-276; c) F. Hsu, G. Park, Z. Guo, Key Residues for the Formation of Aβ42 Amyloid Fibrils, *ACS Omega* **2018**, *3*, 8401-8407.

[2] a) S. Daly, A. Kulesza, F. Poussigue, A. L. Simon, C. M. Choi; G. Knight, F. Chirot, L. MacAleese, R. Antoine, P. Dugourd, *Chem. Sci.* **2015***, 6*, 5040-5047. Correction in: *Chem Sci.* **2016**, *7*, 1609-1610; b) J. Jarvet, P. Damberg, K. Bodell, L. E. G. Eriksson, A. Graslund, *J. Am. Chem. Soc.* **2000**, *122*, 4261-4268; c) J. Jarvet, P. Damberg, J. Danielsson, I. Johansson, L. E. Eriksson, A. Gräslund, *FEBS Lett.* **2003**, *555*, 371-374.

[3] a) T. A. Enache, A. M. Chiorcea-Paquim, A. M. Oliveira-Brett, Amyloid Beta Peptide VHHQ, KLVFF, and IIGLMVGGVV Domains Involved in Fibrilization: AFM and Electrochemical Characterization, *Anal. Chem.* **2018**, *90*, 2285-2292; b) R. Liu, C. McAllister, Y. Lyubchenko, M. R. Sierks, Residues 17-20 and 30-35 of beta-amyloid play critical roles in aggregation, *J. Neurosci. Res.* **2004**, *75*, 162-171.

[4] S. J. Wood, R. Wetzel, J. D. Martin, M. R. Hurle, Prolines and Amyloidogenicity in Fragments of the Alzheimer's Peptide beta/A4, *Biochemistry* **1995**, *34*, 724-730.

[5] a) P. E. Fraser, J. T. Nguyen, W. K. Surewicz, D. A. Kirschner, pH-dependent structural transitions of Alzheimer amyloid peptides. *Biophys. J.* **1991***, 60*, 1190-1201; b) P. Mandal, N. Eremina, A. Barth, Formation of Two Different Types of Oligomers in the Early Phase of pH-Induced Aggregation of the Alzheimer Aβ(12-28) Peptide, *J. Phys. Chem. B.* **2012***, 116*, 12389–12397.

[6] a) Daly, S.; Kulesza, A.; Poussigue, F.; Simon, A. L.; Choi C. M.; Knight, G.; Chirot, F.; MacAleese, L.; Antoine, R.; Dugourd, P. Conformational changes in amyloid-beta (12-28) alloforms studied using action-FRET, IMS and molecular dynamics simulations. *Chem. Sci.* **2015***, 6*, 5040-5047. Correction in: *Chem Sci.* **2016**, *7*, 1609-1610. b) Jarvet, J.; Damberg, P.; Bodell, K.; Eriksson, L. E. G.; Graslund, A. Reversible Random Coil to β-Sheet Transition and the Early Stage of Aggregation of the Aβ(12−28) Fragment from the Alzheimer Peptide. *J. Am. Chem. Soc.* **2000**, *122*, 4261-4268, c) Jarvet, J.; Damberg, P.; Danielsson, J.; Johansson, I.; Eriksson, L. E.; Gräslund, A. A left-handed 3(1) helical conformation in the Alzheimer Abeta(12-28) peptide. *FEBS Lett.* **2003**, *555*, 371-374.

[7] a) Simona, F.; Tiana, G.; Broglia, R. A.; Colombo, G. Modeling the alpha-helix to beta-hairpin transition mechanism and the formation of oligomeric aggregates of the fibrillogenic peptide Abeta(12-28): insights from all-atom molecular dynamics simulations. *J. Mol. Graphics Modell.* **2004**, *23*, 263–273; b) Baumketner, A.; Shea, J. E. Folding landscapes of the Alzheimer amyloid-beta(12-28) peptide. *J. Mol. Biol.* **2006**, *362*, 567– 579, c) Cao, Z. X.; Liu, L.; Zhao, L. L.; Wang, J. H. Effects of Different Force Fields and Temperatures on the Structural Character of Abeta (12–28) Peptide in Aqueous Solution. *Int. J. Mol. Sci.* **2011**, *12*, 8259–8274.

[8] Le, T. N.; Poully, J. C.; Lecomte, F.; Nieuwjaer, N.; Manil, B.; Desfrancois, C.; Chirot, F.; Lemoine, J.; Dugourd, P.; van der Rest, G.; Gregoire G. Gas-phase structure of amyloid-β (12-28) peptide investigated by infrared spectroscopy, electron capture dissociation and ion mobility mass spectrometry. *J. Am. Soc. Mass Spectrom.* **2013**, *24*, 1937–1949.

Chemical compounds.

Dimethyl sulfoxide (DMSO); N-(2-hydroxyethyl) piperazine-N′-(2-ethanesulfonic acid) (HEPES); glycine; Tris(hydroxymethyl)-aminomethane (Tris); TFA, Trifluoroacetic acid and dimethyl sulfoxide (DMSO) were acquired from Sigma Aldrich. All commercially available solvents and reagents were used without further purification. *N,N´*-Dimethylformamide (puriss. p.a., >99.8%) (DMF), 1-hydroxybenzotriazol (HOBt) for peptide synthesis, >99.8%) (NMP), dichloromethane (reagent grade, >99.5%) (DCM), methanol (reagent grade, >99.5%), trifluoroacetic acid (reagent grade, >98%) (TFA), piperidine (reagent grade, >98%), and *N,N´*-diisopropylcarbodiimide (99%) (DIC), Triisopropylsilane (TIS), were purchased from standard sources.

The small-molecule compound iododiflunisal (IDIF), an iodinated analogue of the NSAID diflunisal was synthesized in our lab IQAC-CSIC following our reported procedures.[1]The NSAIDs diflunisal (DIF) and *N*-(3,5-dichlorophenyl)anthranilic (DCPA) were from Sigma Aldrich. (diflunisal, D3281; DCPA, D8942; purity ≥98%). The small-molecule *N*-(3,5-difluorophenyl)anthranilic (DFPA) was prepared in our lab as previously described.[2] Purity of all final compounds was proved to be ≥95% by means of HPLC, HR-MS, and NMR techniques. Stocks of compounds assayed as small molecule ligands were dissolved in DMSO (ACS spectrophotometric grade, Sigma 154938) to a final 10 mM concentration. Working solutions of ligands were prepared by taking an aliquot of 50 µl of the DMSO (5%) stock solution and diluting it with 950 µl of buffer A (25 mM HEPES buffer, 10 mM glycine, pH 7.4 was prepared in the absence of salt), ratio (1:20), equivalent to a 500 µM concentration of ligand.

1. T. Mairal, J. Nieto, M. Pinto, M. R. Almeida, L. Gales, A. Ballesteros, J. Barluenga, J. J. Pérez, J. T. Vázquez, N. B. Centeno, M. J. Saraiva, A. M. Damas, A. Planas, G. Arsequell, G. Valencia, Iodine atoms: a new molecular feature for the design of potent transthyretin fibrillogenesis inhibitors. *PLoS One* **2009***, 4*, e4124.

2. C. A. Ribeiro, M. J. Saraiva, I. Cardoso, Stability of the Transthyretin Molecule as a Key Factor in the Interaction with A-Beta Peptide-Relevance in Alzheimer's Disease. PloS ONE **2012**, 7 (9):e45368.

Recombinant wild-type human (wt rhTTR) production and purification

Recombinant wild-type hTTR was produced using a pET expression System. Human wild type rhTTR gene was cloned into a pET expression system and transformed into *E. coli* BL21(DE3) Star. The phTTRwt-I/pET-38b(+) plasmid was kindly provided by Prof. Antoni Planas (IQS, URL). The expressed protein only contains an additional methionine on the *N*-terminus if compared to the mature natural human protein sequence. wt rhTTR protein was expressed in *E. coli* BL21-(DE3) cells harbouring the corresponding plasmid. Expression cultures in 2xYT rich medium containing 100 µg/mL kanamycin were grown at 37 °C to an optical density (at 600 nm) of 4 (OD600≈4), then induced by addition of IPTG (1 mM final concentration), grown at 37 °C for 20 h, and harvested by centrifugation at 4 ºC, 10000 rpm for 10 min and resuspended in cell lysis buffer (0,5 M Tris-HCl, pH 7.6). Cell disruption and lysis were performed by French press followed by a sonication step at 4ºC. Cell debris were discarded after centrifugation at 4ºC, 11000 rpm for 30 min. Intracellular proteins were fractionated by ammonium sulfate precipitation in three steps. Each precipitation was followed by centrifugation at 12ºC, 12500 rpm for 30 min. The pellets were analysed by SDS-PAGE (14% acrylamide). The TTR-containing fractions were resuspended in 20 mM Tris-HCl, 0.1 M NaCl, pH 7.6 (buffer A) and dialyzed against the same buffer. It was purified by Ion exchange chromatography using a Q-Sepharose High Performance (Amersham Biosciences) anion exchange column and eluting with a NaCl linear gradient using 0.1M NaCl in 20 mM Tris-HCl pH 7.6 buffer A to 0.5 M NaCl 20 mM Tris-HCl pH 7.6 (buffer B). All TTR-enriched fractions were dialyzed against deionized water in three steps and were lyophilized. The protein was further purified by gel filtration chromatography using a Superdex 75 prep grade resin (GE Healthcare Bio-Sciences AB) and eluting with 20 mM Tris pH 7.6, 0.1 M NaCl. Purest fractions were combined and dialyzed against deionized water and lyophilized. The purity of protein preparations was >95% as judged by SDS-PAGE. Average production yields were 150-200 mg of purified protein per liter of culture. Protein concentration was determined spectrophotometrically at 280 nm using calculated extinction coefficient value of 17780 M-1.cm-1 for wtTTR. The protein was stored a -20ºC (See Scheme S1). A full description of this procedure will be published elsewhere.

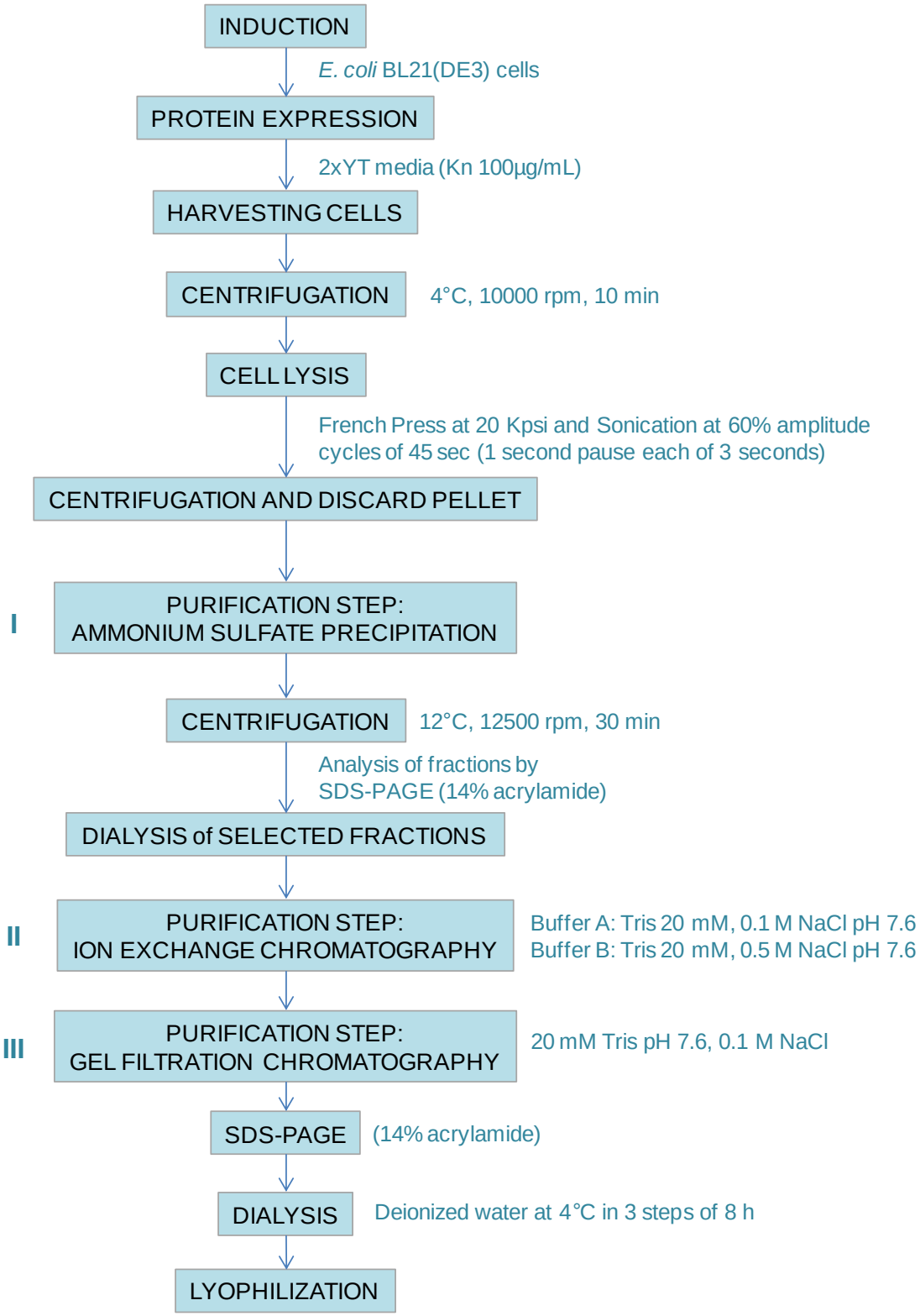

Scheme S1. Expression and purification of wild type transthyretin protein (wtTTR).

Protein expression and purification

Following the protocol shown in Scheme S1 we obtained 150 mg of wtTTR/L culture. Purity of wt rhTTR was checked by SDS-PAGE and mass spectrometry (MS). Our sequence has a molecular mass of 13910 Da and contains an additional methionine of 149,21 Da on the *N*-terminus, compared to the mature natural human protein sequence which has an average molecular mass of 13762 Da.) (See Figure S1). As shown in the Figure the wt rhTTR obtained has > 98% of purity after the last purification by size exclusion chromatography (SEC).

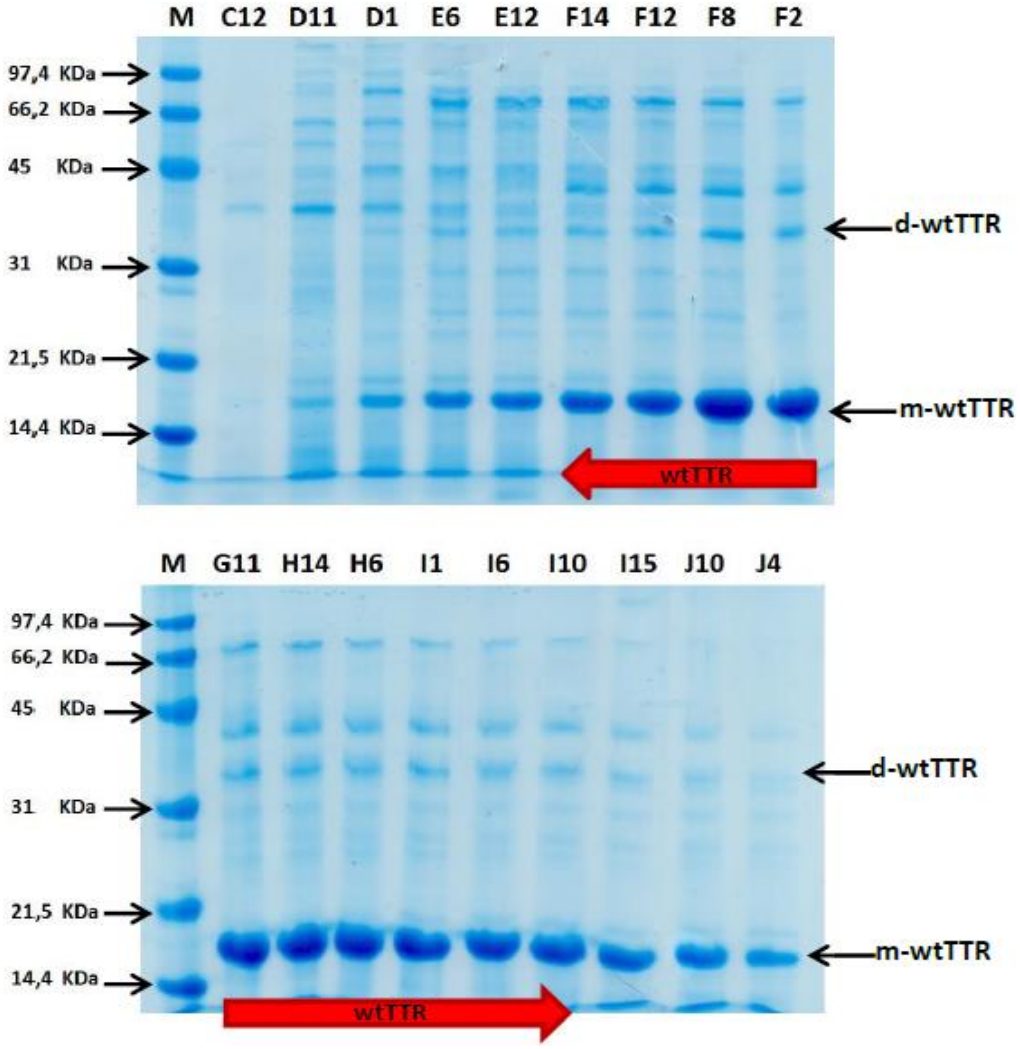

Figure S1. SDS-PAGE (14% acrylamide) of wt rhTTR. Selected fractions are shown with arrows in red.

Characterization of wtTTR by MALDI-TOF MS

Protein solution and sinapinic acid (SA) matrix (saturated solution of SA in 30:70 v/v acetonitrile: water at 0.1 % TFA) were mixed at 1:1 ratio. A volume of 0.5 µL of the previous mixture was deposited into a polished stainless-steel target (Bruker) and allowed to dry. The deposited sample was washed with 0.1 % TFA solution and allowed to dry again. Finally, 0.5 µL of SA matrix were deposited into the washed sample and allowed to dry. Same procedure was done for the Protein Standard Calibration I solution (Bruker). The target was introduced in a Microflex MALDI-TOF (Bruker), spectra was acquired in lineal mode (Flex Control, Bruker) and processed (Flex Analysis, Bruker). External calibration with Protein Standard Calibration I (Bruker) was performed.

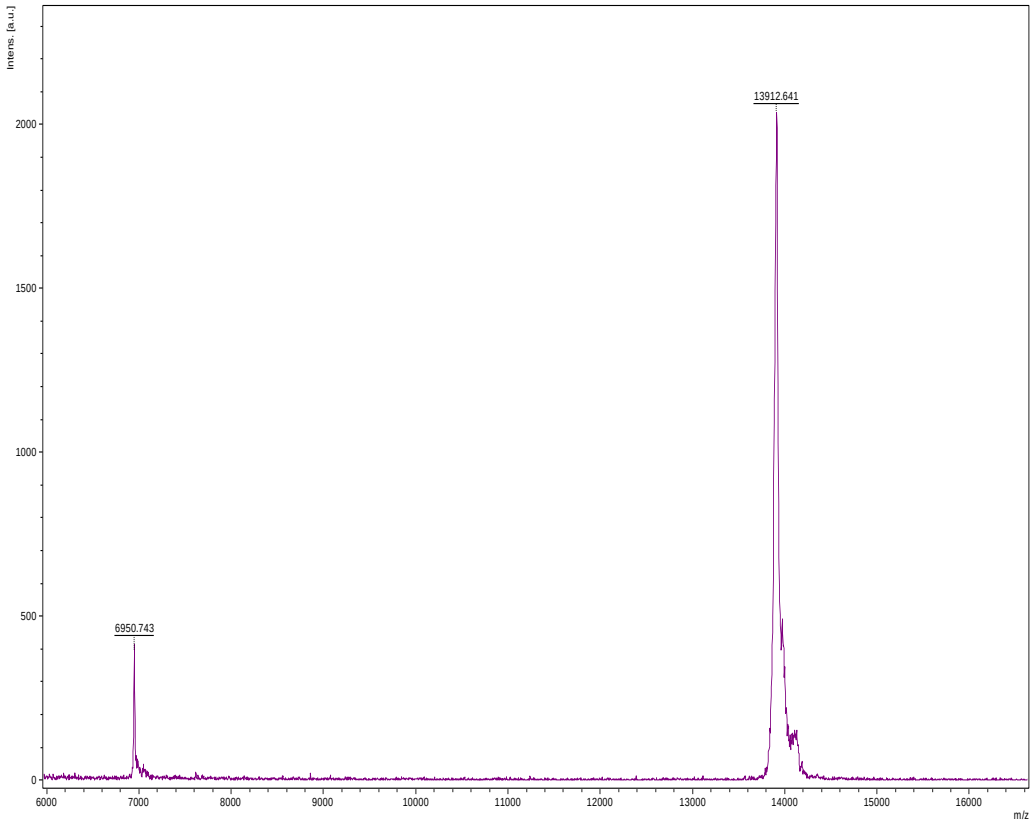

Figure S2. MALDI-ToF MS. Mass spectrum of wtTTR, both unmodified form 13915 Da and Cys-10 modified form (S-GSH) with 14202 Da. The MS spectrum also shows signal of $(M+2H)^{2+}$.

Turbidity assay

The following stock solutions were used: Buffer A: 25 mM HEPES buffer, 10 mM glycine, pH 7.4 was prepared in the absence of salt. Protein (TTR) stock: 9,5 mg/mL (170 μM) in 25 mM HEPES buffer, 10 mM glycine, pH 7.4 and 5% DMSO (final concentration) was prepared in the absence of salt (buffer A). For the *Aβ peptide stock*: 0,4 mg/mL (200 μM) in 25 mM HEPES buffer, 10 mM glycine, pH 7.4 and 5% DMSO (final concentration). For the small-molecule compound IDIF, a first solution of 3,76 mg/mL (10 mM) in DMSO was prepared. The final stock of the small-molecule IDIF was prepared by mixing 50 µL of the previous DMSO solution with 950 µL of buffer A (the final concentration of 5% DMSO).

First, the small-molecule compound and TTR complex was formed. To this end, 60 µL of TTR stock was dispensed into the wells of a 96-well microplate. 40 µL of small-molecule stock was added to give final concentrations of 100 µM. The plate was introduced in the microplate reader (SpectraMax M5 Multi-Mode Microplate Readers, Molecular Devices Corporation, California, USA) and incubated for 1h at 37 °C with orbital shaking 15 s every 30 min. Then, 100 μL of Aβ solution was added to the well to give a final concentration of 100 μM.

Other wells of the 96-well microplate are filled with: a) Buffer alone: 200 µL of buffer A solution was added to the well; b) Negative control of Aβ aggregation: 200 µL of Aβ(1-11) stock solution in buffer A was dispensed into the wells; c) Testing TTR aggregation: 60 µL of TTR stock were dispensed into the wells of a 96-well microplate and 140 µL of buffer A were added; d) For the Aβ(12-28) aggregation: 100 µL of Aβ(12-28) stock solution is dispensed into the wells and 100 µL of buffer A were added.

The plate was incubated at 37 °C in a thermostated microplate reader with orbital shaking 15 s every minute for 30 min. The absorbance at 340 nm was monitored for 6 h at 30 min intervals. Data were collected and analyzed using Microsoft Excel software. All assays were done in duplicate.

$$RA(\%) = \left[1 - \left(\frac{Abs_c}{Abs_{\mathrm{A\beta}} + Abs_c}\right)\right] * 100 \qquad (1)$$

The parameter monitored in this assay was used to calculate the percent reduction of formation of aggregates (RA %) according to equation 1, where $Abs_{A\beta}$ and Abs_c are the final absorbance of the samples, in the absence or in the presence of the small-molecule compound/TTR complex; respectively.

Turbidity assay: stock solutions

Other wells of the 96-well microplate are filled with: a) Buffer alone: 200 µL of buffer A solution was added to the well; b) Negative control of Aβ aggregation: 200 µL of Aβ(1-11) stock solution in buffer A was dispensed into the wells; c) Testing TTR aggregation: 60 µL of TTR stock were dispensed into the wells of a 96-well microplate and 140 µL of buffer A were added; d) For the Aβ(12-28) aggregation: 100 µL of Aβ(12-28) stock solution is dispensed into the wells and 100 µL of buffer A were added.

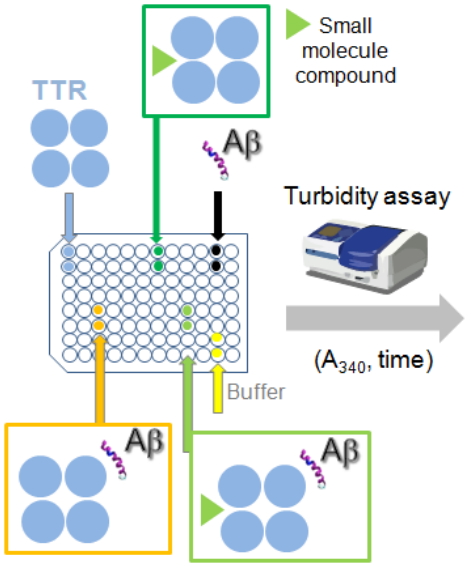

Scheme S2. Representation of the microplate with different samples before Turbidity assay.

Preliminary experiments

Turbidity assays: Aggregation kinetics of Aβ(12-28)

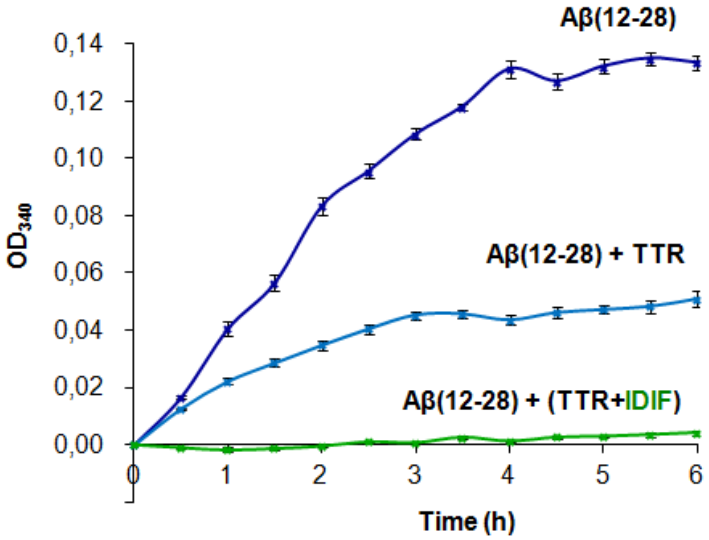

Figure S3. Aβ(12-28) aggregation monitored by turbidity assay at 37 °C over 6 h at pH 7.4 in 25 mM HEPES buffer, 10 mM glycine and 5% DMSO (final concentration) at 37 ºC. Aggregation kinetics of: Aβ(12-28) alone (100 µM) (dark blue line); Aβ(12-28) (50 µM) in the presence of TTR (50 µM) (blue line) (ratio 2:1); and Aβ(12-28) (100 µM) in the presence of the complex TTR/IDIF (TTR 50 µM; IDIF 100 µM) (ratio 2:1:2) (green line). Samples were assayed in duplicate and are representative of three different replicates (n=6). Negative controls (buffer solutions) are not shown.

Design of experiments (DoE)

Factorial designs are one of the most important DoE because they produce efficient experiments that allow observation of responses to one factor at different levels of other factors in the same experiment.[1,2] They allow the investigation of the main effect of factors but also their interactions (when factors do not act independently of others). Factors are types of treatments (quantitative or qualitative) which have several levels. The Factorial design consists of all possible combinations of the levels of several factors. These combinations (runs) are defined and randomly ordered and realized in the laboratory, obtaining therefore the value of the response variable (Y) for each factor's combination. Behind the Factorial design a statistical model is defined: an Analysis of Variance (ANOVA) model. Several sums of squares are constructed to estimate the effects of factors and their interactions on Y. Tests of hypotheses about factor effects and their interactions are also calculated to determine the statistical significance. More than one replicate of each combination of the experiment is needed to estimate the variance error. To reduce the experimental error variation a method called blocking can achieve more precision. Blocking consists of introducing an additional factor called block which is an external variable to the treatments and that creates a stratification of the runs into homogeneous groups. The block effect can be also introduced into the statistical model and be estimated. The statistical software used was JMP 12.1.0 (SAS Institute).[3]

1. Kuehl, R. O. *Design of experiments: statistical principles of research design and analysis*. 2nd ed.; Duxbury/Thomson Learning Pacific Grove: CA, 2000.
2. Box, G. E. P.; Stuart Hunter, J.; Hunter, W.G. *Statistics for Experimenters: Design, Innovation, and Discovery*. 2nd ed.; Wiley-Interscience: New Jersey, 2005.
3. JMP ®, Version 12.1.0. SAS Institute Inc., Cary, NC, USA.

Method development and optimization

The variable to be maximized has been the absorbance. Preliminary investigations were carried out to select initial analysis conditions, taking into account that temperature and ionic strength may have a nonlinear effect on the fibril formation, we have considered these two factors in a two–level design, the temperature at 37 ºC and 40 °C and the ionic strength ([NaCl]) at 0 and 100 mM. The concentration was considered at three levels 50, 100 and 200 µM, because we wish identified the sensitivity for our method. The UV absorption maxima for Aβ-peptide fibril formation is achieved at 340, 360 and 405 nm. The flow layout of a Design of Experiments for method development and data analysis is illustrated in **Scheme S3**.

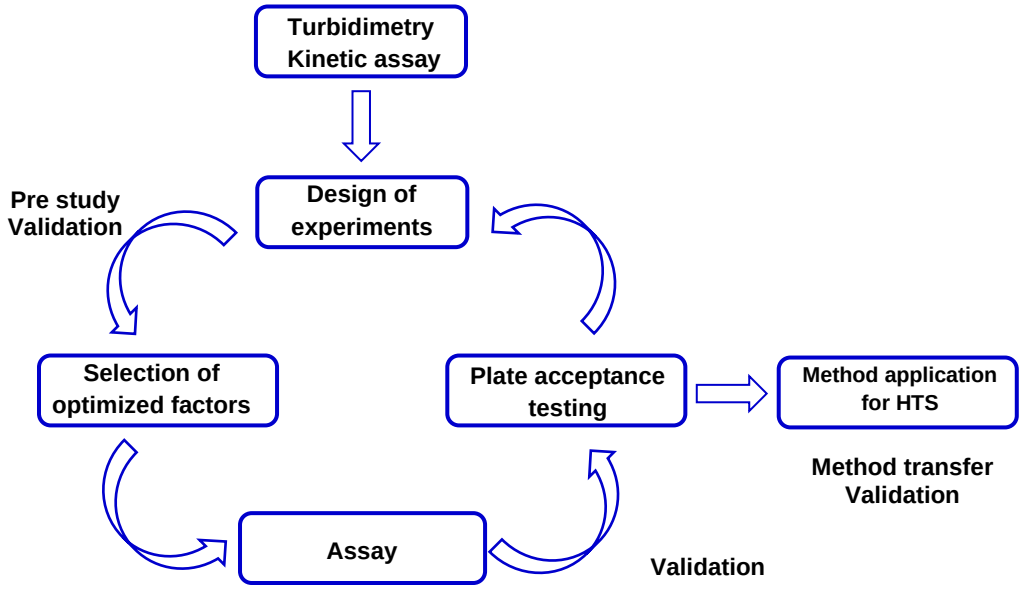

Scheme S3. Flow layout in Design of Experiments (DoE).

Spectral scanning of Aβ(12-28)

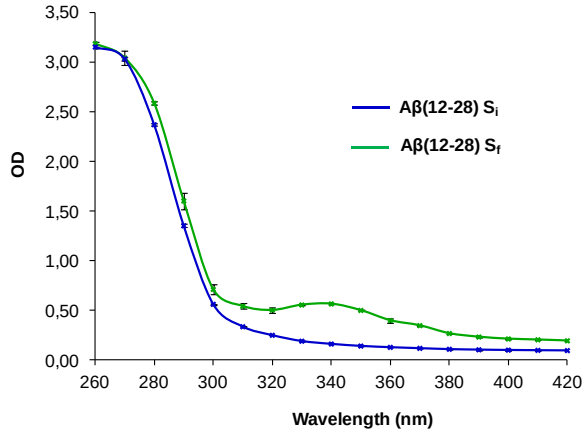

Figure S4. Spectral scanning of a 200 μM solution of Aβ(12-28). The blue trace corresponds to the initial clean solution (S_i) and the green to the same solution after 6h at 37ºC that became turbid (S_f). Three different experiments were conducted with duplicate samples (n=6).*** Studies performed at pH 7.4 in 25 mM HEPES buffer, 10 mM glycine and 5% DMSO (final concentration) at 37 ºC.

Factorial design by applying JMP software

A factorial design was applied in our analysis (Table S1). Initial number of experiments was 48, creating the matrix design described in Table S2. We modified the initial matrix design adding a column to study the effect of different batches of peptide, as a block effect. Randomizing all runs we realized the experiments in the laboratory and the measured values of absorbance for each run were obtained (Table S2). In some of these combinations (3-+, 3+- and 3++) it was not possible to obtain the absorbance.

The Table S3 shows the initial 48 numbers of experiments, plus 2 replicates that were explored for the 2-- combination on the 2nd level of the block (factors' selected conditions). To confirm results at these selected set of conditions, six more runs (n=6) were randomly done and analyzed, in order to ensure reproducibility of the previous results.

Analysis of variance (ANOVA) results of the adjusted model are shown in Table S4. Results shown as the model is globally statistically significant ($p < 0.0001$). Goodness of fit measures as R squared values (RSq), the root mean square error (RMSE) and graphs between the original absorbance and predicted absorbance were analyzed. The significance of the parameters in the model is shown in Table S2.

It was found that all the main factors (concentration, ionic strength and temperature) and the interactions between concentration and the other two factors were statistically significant but not the temperature versus ionic strength interaction. As expected, the block factor was not statistically significant (Table S5).

Table S1. Design levels of factors.

Factor[1]	Low level	High level	Midpoint
Concentration (μM)	50	200	100
Temperature (°C)	37	40	*
Ionic strength (mM of NaCl)	0	100	*

[1]The initial numbers of experiments were 48.

Table S2. Matrix design of the experimental runs.

Run	Concentration	Temperature	Ionic Strength	Block
1−−	50	37	0	1
1−+	50	37	100	1
1+−	50	40	0	1
1++	50	40	100	1
2−−	100	37	0	1
2−+	100	37	100	1
2+−	100	40	0	1
2++	100	40	100	1
3−−	200	37	0	1
3−+	200	37	100	1
3+−	200	40	0	1
3++	200	40	100	1
1−−	50	37	0	1
1−+	50	37	100	1
1+−	50	40	0	1
1++	50	40	100	1
2−−	100	37	0	1
2−+	100	37	100	1
2+−	100	40	0	1
2++	100	40	100	1
3−−	200	37	0	1
3−+	200	37	100	1
3+−	200	40	0	1
3++	200	40	100	1
1−−	50	37	0	2
1−+	50	37	100	2
1+−	50	40	0	2
1++	50	40	100	2
2−−	100	37	0	2
2−+	100	37	100	2
2+−	100	40	0	2
2++	100	40	100	2
3−−	200	37	0	2
3−+	200	37	100	2
3+−	200	40	0	2
3++	200	40	100	2
1−−	50	37	0	2
1−+	50	37	100	2
1+−	50	40	0	2
1++	50	40	100	2
2−−	100	37	0	2
2−+	100	37	100	2
2+−	100	40	0	2

2++	100	40	100	2
3−−	200	37	0	2
3−+	200	37	100	2
3+−	200	40	0	2
3++	200	40	100	2

Table S3. JMP data table of Complex Factorial Design runs with their corresponding measured responses of absorbance.

Run[1]	Concentration	Temperature	Ionic Strength	Block	Absorbance
1−−	50	37	0	1	0,0449
1−+	50	37	100	1	0,0497
1+−	50	40	0	1	0,0673
1++	50	40	100	1	0,0656
2−−	100	37	0	1	0,1197
2−+	100	37	100	1	0,1206
2+−	100	40	0	1	0,1152
2++	100	40	100	1	0,1239
3−−	200	37	0	1	0,1617
3−+	200	37	100	1	*
3+−	200	40	0	1	*
3++	200	40	100	1	*
1−−	50	37	0	1	0,0457
1−+	50	37	100	1	0,0486
1+−	50	40	0	1	0,0552
1++	50	40	100	1	0,0592
2−−	100	37	0	1	0,1188
2−+	100	37	100	1	0,1193
2+−	100	40	0	1	0,1134
2++	100	40	100	1	0,1208
3−−	200	37	0	1	0,1692
3−+	200	37	100	1	*
3+−	200	40	0	1	*
3++	200	40	100	1	*
1−−	50	37	0	2	0,0555
1−+	50	37	100	2	0,0516
1+−	50	40	0	2	0,0557
1++	50	40	100	2	0,0581
2−−	100	37	0	2	0,114
2−+	100	37	100	2	0,126
2+−	100	40	0	2	0,1256
2++	100	40	100	2	0,1292
3−−	200	37	0	2	0,1773
3−+	200	37	100	2	*
3+−	200	40	0	2	*
3++	200	40	100	2	*

1−−	50	37	0	2	0,059
1−+	50	37	100	2	0,0548
1+−	50	40	0	2	0,0565
1++	50	40	100	2	0,0591
2−−	100	37	0	2	0,1132
2−+	100	37	100	2	0,1249
2+−	100	40	0	2	0,1283
2++	100	40	100	2	0,1304
3−−	200	37	0	2	0,1716
3−+	200	37	100	2	*
3+−	200	40	0	2	*
3++	200	40	100	2	*
2−−	100	37	0	2	0,125
2−−	100	37	0	2	0,1219
2−−	100	37	0	2	0,1264
2−−	100	37	0	2	0,1237
2−−	100	37	0	2	0,126
2−−	100	37	0	2	0,1278

[1]Original runs (48) plus 6 additional replicates.

Table S4. Analysis of Variance (ANOVA) results.

Source of variation	Sum of Squares	Degrees of Freedom	Mean Square	F Ratio	Prob > F
Model	0,057	7	0,0082	67,8353	< 0,0001*
Error	0,0044	30	0,00012		
Total	0,061	37			

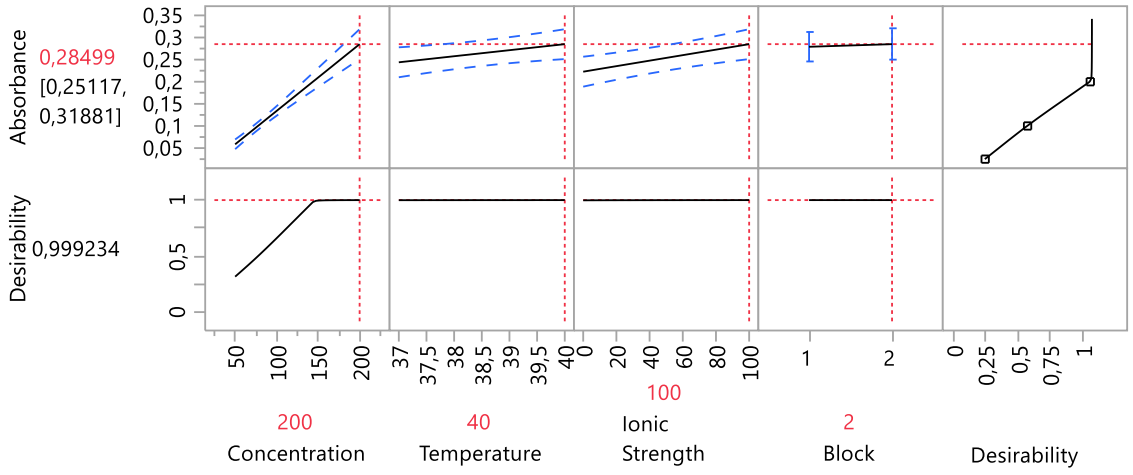

Figure S5. Prediction profile and desirability plot in the complex factorial design.

In the prediction profile JMP software automatically adjusts the graph to display the optimal settings at which the best response of the absorbance is obtained. The factors temperature and ionic strength did have a significant but poor effect on the absorbance response. Block factor was not statistically significant.

Table S5. Analysis of variance results for the different factors and their interactions in the turbidimetric assay.

Source of variation	Log Utility	p-value[1]
Concentration	16,444	0,000
Concentration*Ionic strength	2,917	0,001
Ionic Strength	1,713	0,019
Temperature	1,698	0,020
Concentration*Temperature	1,368	0,043
Block effect	0,974	0,106
Temperature*Ionic strength	0,018	0,959

[1] Statistically significant factors and interactions are those whose p-value < 0.05.

Turbidity assays: Aggregation kinetics of Aβ(12-28) and Aβ(1-42) peptides up to 18 h:

a) in the presence and absence of IDIF; b) in the presence of TTR; and c) in the presence of TTR + IDIF

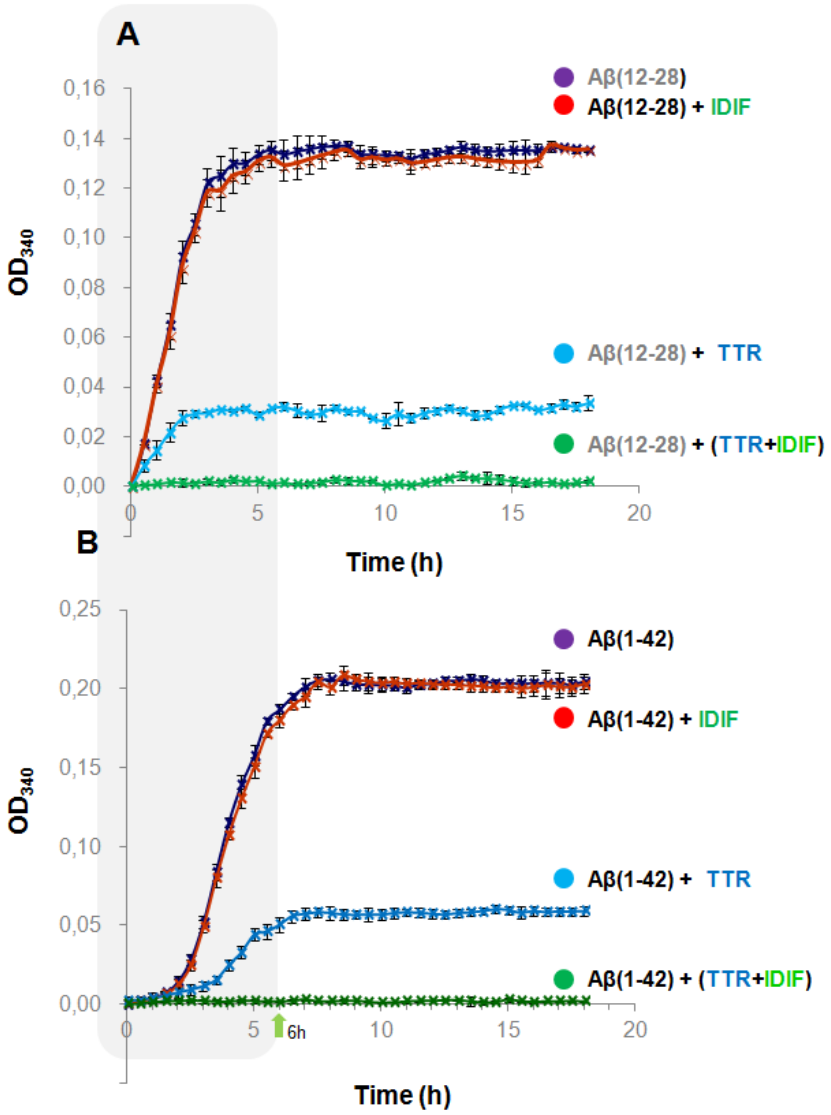

Figure S6:

A) Inhibition of Aβ(12-28) aggregation monitored by turbidity assay at 37 °C over 18 h. Aggregation kinetics of: Aβ(12-28) alone (dark violet line); Aβ(12-28) in the presence of IDIF (red line); Aβ(12-28) in the presence of TTR (blue line); and Aβ(12-28) in the presence of the complex TTR/IDIF (green line).

B) Inhibition of Aβ(1-42) aggregation monitored by turbidity assay at 37 °C over 18 h. Aggregation kinetics of: Aβ(1-42) alone (dark violet line); Aβ(1-42) in the presence of IDIF (red line); Aβ(1-42) in the presence of TTR (blue line); and Aβ(1-42) in the presence of the complex TTR/IDIF (green line). Samples were assayed in duplicate and are representative of three different replicates (n=6). Negative controls (buffer solutions) are not shown. (Fig. S6B was included in the Supporting Information from Cotrina et al. *J. Med. Chem.* 2020, **63**, 3205-3214).

Turbidity assays: aggregation kinetics of Aβ(1-42) with Aβ(12-28) at two different concentrations followed by Turbidity assays.

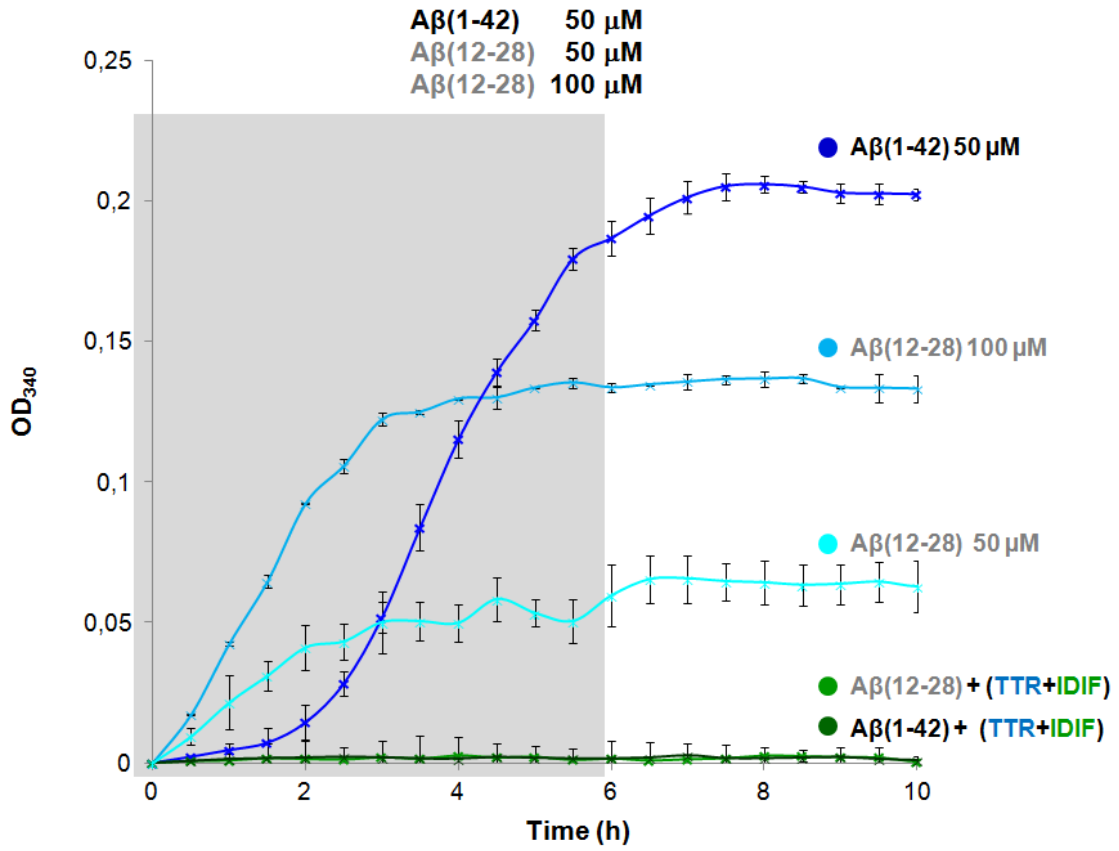

Figure S7: Aggregation kinetics of Aβ peptides by Turbidity assay at 37 °C over 10 h.: Aβ(1-42) alone (dark blue line); Aβ(12-28) (100 μM) (light blue line); Aβ(12-28) (50 μM) (bright blue line); and Aβ(1-42) and Aβ(12-28) in the presence of the complex TTR/IDIF (green lines). Samples were assayed in duplicate and are representative of three different replicates (n=6). Negative controls (buffer solutions) are not shown

A similar comparison of the aggregation kinetics of different Aβ peptides, including Aβ(12-28), was reported using ThT assays with Aβ(1-40), Aβ(1-42), and Aβ(12-28) at 100 μM (Sadowski et al. 2004, page 941).

M. Sadowski, J. Pankiewicz, H. Scholtzova, J. A. Ripellino, Y. Li, S. D. Schmidt, P. M. Mathews, J. D. Fryer, D. M. Holtzman, E. M. Sigurdsson, T. Wisniewski. A synthetic peptide blocking the apolipoprotein E/beta-amyloid binding mitigates beta-amyloid toxicity and fibril formation in vitro and reduces beta-amyloid plaques in transgenic mice. *Am. J. Pathol.* **2004**, *165*, 937-948.

Thioflavin-T (ThT) fluorescence assays

The robustness of our turbidimetry-based method was further validated on the basis of comparative by Thioflavin-T (ThT) fluorescence assays on the same system. The ThT fluorescence was monitored at 37 °C using Gemini XPS plate reader (Molecular Devices) at an excitation wavelength of 440 nm and an emission wavelength of 490 nm. Thioflavin-T (ThT) was dissolved in 25 mM HEPES buffer, 10 mM glycine, pH 7.4 and 5 % DMSO to a final concentration of 10μM. Aggregation of Aβ(1-42) 20 μM was performed in the presence of 10 μM ThT. All solutions were dissolved in the same buffer. TTR was added to a final concentration of 10 μM. IDIF was added to a final concentration of 20 μM. For the ternary complex, TTR was incubated first with IDIF for 1h, then Aβ(12-28) was added. The final volume was 200 μL for all samples. Fluorescence intensity at 490 nm of each sample was monitored after each 2h for 8h, and then at 21h. Measurements were performed as independent triplicates. Recorded values were averaged and background measurements (buffer containing 25 μM ThT) were subtracted. Measurements were performed as independent triplicates. Recorded values were averaged and background measurements (buffer containing 25 μM ThT) were subtracted.

Thioflavin T studies: Aggregation kinetics of Aβ(12-28) and Aβ(1-42)

Aggregation kinetics of Aβ(12-28) (Figure S8A) and Aβ(1-42) peptide (Figure S8B): alone; in the presence of TTR or in the presence of TTR stabilized with different small-molecule compounds.

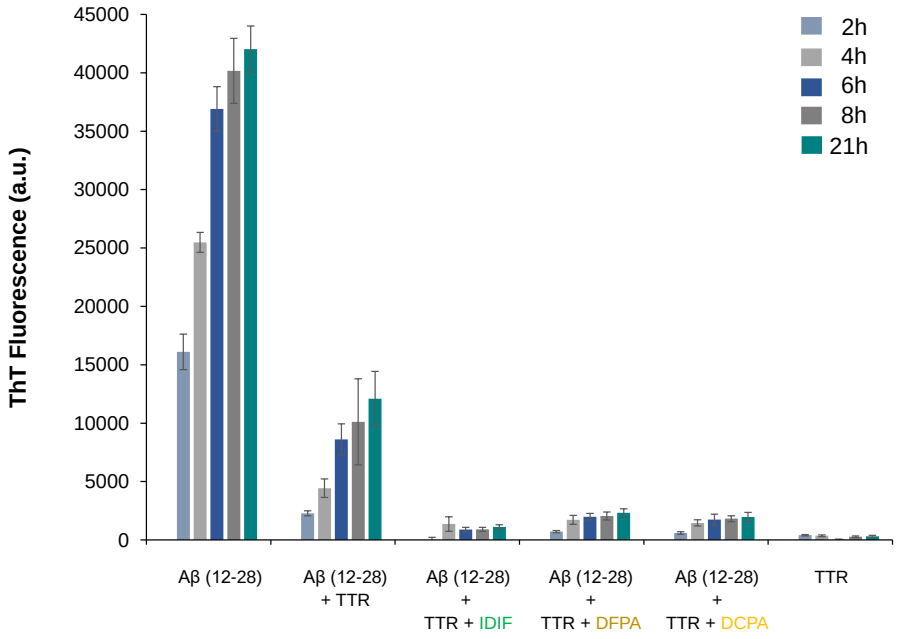

Figure S8A: ThT assays of the aggregation of Aβ(12-28) alone (50 μM), in complex with TTR (25 μM), or in complex with TTR stabilized with different small compounds (50 μM), (TTR/IDIF, TTR/DCPA and TTR/DFPA). ThT fluorescence was measured at 37 ºC each 10 min for 3h, then each 20 min from 3 h to 6 h, and then at 8 h. Samples were assayed in duplicate and are representative of three different replicates (n=6). Negative controls (buffer solutions) are not shown.

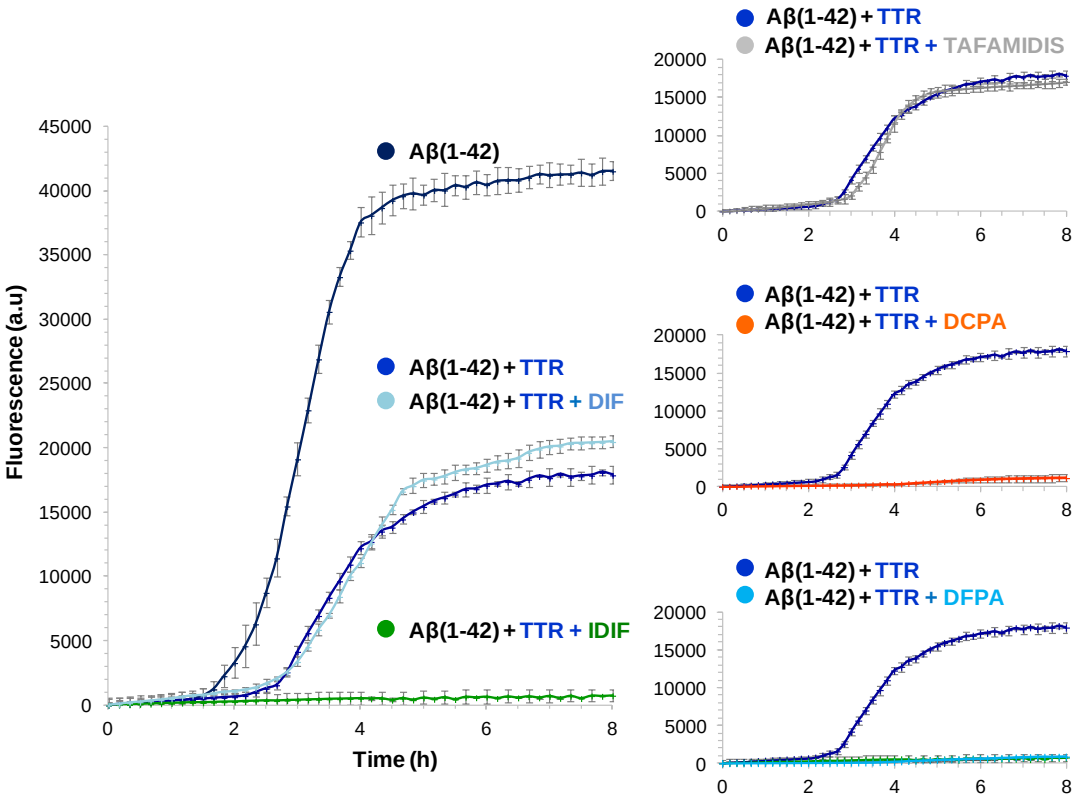

Figure S8B: ThT assays of the aggregation of Aβ(1-42) alone (20 μM), in complex with TTR (10 μM), or in complex with TTR stabilized with different small compounds (20 μM), (TTR/IDIF, TTR/DIF, TTR/Tafamidis, TTR/DCPA and TTR/DFPA). ThT fluorescence was measured at 37 ºC each 10 min for 3h, then each 20 min from 3 h to 6 h, and then at 8 h. Samples were assayed in duplicate and are representative of three different replicates (n=6). Negative controls (buffer solutions) are not shown.

Transmission Electron Microscopy (TEM)

Aβ(12-28) peptide (100 μM), alone or with TTR (20 μM) (alone or pre-incubated with IDIF for 1 hour at 37 °C) was incubated at 37 °C for 48 h. For visualization by TEM, 5 μl sample aliquots were absorbed to carbon-coated collodion film supported on 200-mesh copper grids, for 5 minutes, and negatively stained with 1% uranyl acetate. Grids were exhaustively examined with a JEOL JEM-1400 transmission electron microscope equipped with an Orious Sc1000 digital camera.

Morphological analysis of aggregates and of their cell toxicity: TEM studies

It is well established that Aβ peptide, in particular its oligomeric form, is toxic to cells leading to apoptosis and cellular death. Previous work has demonstrated that TTR protects against this neurotoxicity.[1-3]

1. R. Costa, A. Gonçalves, M. J. Saraiva, I. Cardoso, Transthyretin binding to A-Beta peptide--impact on A-Beta fibrillogenesis and toxicity. *FEBS Lett.*, 2008, **582**, 936-942.
2. L. Nilsson, A. Pamrén, T. Islam, K. Brännström, S. A. Golchin, N. Pettersson, I. Iakovleva, L. Sandblad, A. L. Gharibyan, A. Olofsson, Transthyretin Interferes with Aβ Amyloid Formation by Redirecting Oligomeric Nuclei into Non-Amyloid Aggregates. *J. Mol. Biol.* 2018**, 430**, 2722-2733.
3. S. A. Ghadami, S. Chia, F. S. Ruggeri, G. Meisl, F. Bemporad, J. Habchi, R. Cascella, C. M. Dobson, M. Vendruscolo, T. P. J. Knowles, F. Chiti, Transthyretin inhibits primary and secondary nucleation of amyloid-β peptide aggregation and reduces the toxicity of its oligomers. *Biomacromolecules*, 2020, **21**, 1112-1125.

TEM studies: Aβ(12-28) in the presence of TTR and of the TTR/IDIF complex.

(reported in Cotrina et al. *J. Med. Chem.* **63**, *6*, 3205-3214 (2020).

To assess the structure of the Aβ(12-28) species generated in the presence of TTR and of the TTR/IDIF complex, we performed a morphological analysis by transmission electron microscopy (TEM). The ultrastructural examination confirmed the known facts [perhaps reference needed] that after 48 h of incubation at 37 °C, Aβ(12-28) formed highly ordered and structured fibrils. In Figure S9A, it is possible to appreciate that fibrils are formed by several protofilaments, laterally assembled (arrow) or twisted over each other (arrowhead). In the presence of TTR only round particles and thin and shorter fibrils were detected (Figure S9B, arrow and arrowhead, respectively). When TTR was previously incubated with IDIF the inhibitory effect was more pronounced and only round and small particles were observed (Figure S9C).

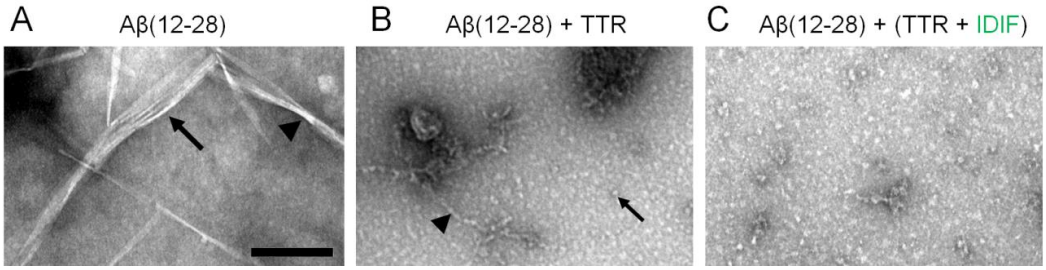

Figure S9. Morphologic assessment by TEM of the influence of TTR on Aβ(12-28) fibrillization. A) Aβ(12-28) after 48 h of incubation at 37 °C; B) Aβ(12-28) in the presence of TTR; and C) Aβ(12-28) in association of TTR/IDIF complex. Scale bar = 200 nm.

Toxicity studies: Aβ(1-42) in the presence of TTR and of the TTR/IDIF complex

Cell culture and caspase-3 assay

SH-SY5Y cells (human neuroblastoma cell line; European Collection of Cell Cultures) were propagated in 25-cm^2 flasks and maintained at 37 °C in a 95% humidified atmosphere and 5% CO_2. Cells were grown in Dulbecco's minimal essential medium supplemented with 10% fetal bovine serum (Gibco BRL). Activation of caspase-3 was measured using the CaspACE fluorimetric 96-well plate assay system (Sigma), following the manufacturer's instructions. Briefly, 10 μM Aβ(1-42) (Genscript) pre-incubated for 48 h at 4 °C with shaking, in F12 media (Gibco BRL) with or without 2 μM TTR (alone or previously incubated with IDIF (20 μM) for 1 h at 37 °C), were added to 80% confluent cells, cultured in 6-well plates, in Dulbecco's minimal essential medium with 1% fetal bovine serum, and further incubated for 24 h, at 37 °C. Subsequently, each well was trypsinized and the cell pellet was lysed in 100 μl of hypotonic lysis buffer (Sigma). Forty μL of each cell lysate were used in duplicates for determination of caspase-3 activation. The remaining cell lysate was used to measure total cellular protein concentration with the Bio-Rad protein assay kit (Bio-Rad), using BSA as standard. Values shown are the mean of duplicates and the experiment was performed twice. Comparison between groups was made using the Student's t-test. A P value of less than 0.05 was considered statistically significant.

As depicted in Figure S10, we confirmed that TTR prevented the noxious effect of the Aβ(1-42) peptide, reducing in about 45% the levels of caspase-3 activation, as compared to the levels produced by the oligomers, although the reduction was not enough to reach the values obtained in the control with media alone. Importantly, TTR stabilized by IDIF was even more potent and caspase-3 levels were reduced in over 60%, as compared to the oligomers. Again, the caspase-3 levels were not as low as the control but were significantly lower than those of measured in cells incubated with Aβ co-incubated with TTR (without IDIF).

Altogether, these results confirm that TTR is a neuroprotective protein, preventing Aβ fibrillogenesis and toxicity, and that TTR performance can be enhanced by small-molecule chaperones of the TTR/Aβ interaction, thus validating our high-throughput assay, and prompting TTR stabilization as a promising therapeutic strategy in AD.

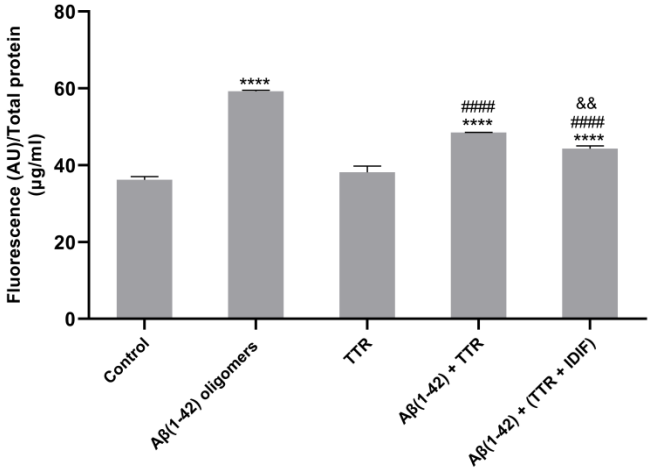

Figure S10. Caspase-3 activation in cell culture. Aβ(1-42) oligomers (10 μM), TTR (2 μM), or Aβ(1-42) co-incubated at 4 °C for 48 h with TTR alone or TTR complexed with IDIF (20 μM) for 1 h at 37 °C, were then added to SH-5YSY cultured cells and further incubated for 24 h at 37 °C. *, # and & denote significance as compared to control, to Aβ(1-42) oligomers and to Aβ(1-42) + TTR, respectively. && $p < 0.01$; **** or #### $P < 0.0001$.

Statistical analysis

The quality of an assay for HTS can be evaluated based on the Z'-factor which reflects the separation in mean values for the high and low controls while taking into consideration the variability within each group.[1] A Z' factor below zero indicates poor quality assay with no separation between the high and low controls. A Z' factor value between 0.5 and 1 indicate an excellent quality assay with large separation between the high and low controls. Preferably, optimized assays have a Z' value above 0.5. The statistical Z'-factor can be calculated using equation 2:

$$Z' = 1 - \frac{3SD\ of\ sample + 3SD\ of\ control}{|mean\ of\ sample - mean\ of\ control|} \qquad (2)$$

where sample is the highest RA% for Aβ(12-28) in presence of the binary complex (TTR+IDIF) or TTR alone, and the control is the Aβ(12-28) aggregation. "Mean" is the mean value of the aggregation after 6 h, and SD is the standard deviation.

1. J. H. Zhang, T. D. Chung and K. R. A. Oldenburg, Simple Statistical Parameter for Use in Evaluation and Validation of High Throughput Screening Assays. *J. Biomol. Screen.*, 1999, **4**, 67-73.

Amyloid peptides.

Aβ(1-42) peptide

In order to prevent the spontaneous formation of aggregates in solution, we have used the depsi-Aβ(1-42) peptide (Genscript, RP10017-1), a chemically-modified β-amyloid (1-42) precursor. This depsipeptide precursor is converted into the corresponding native Aβ(1-42) peptide by a change in pH (1, 2).

References:

1. Y. Sohma, M. Sasaki, Y. Hayashi, T. Kimura, Y. Kiso, Design synthesis of a novel water-soluble Aβ1-42 isopeptide: an efficient strategy for the preparation of Alzheimer's disease-related peptide $A\beta_{1-42}$ via *O–N* intramolecular acyl migration reaction. *Tetrahedron Lett.* **2004**, *45*, 5965-5968.

2. M. Beeg, M. Stravalaci, A. Bastone, M. Salmona, M. Gobbi, A modified protocol to prepare seed-free starting solutions of amyloid-β (Aβ) 1-40 and Aβ 1-42 from the corresponding depsipeptides. *Anal. Biochem.* **2011**, *411*, 297-299.

Other amyloid sequences

The amyloid peptide sequences Aβ(1-11) and Aβ(12-28) were purchased from Bachem AG (Switzerland) as trifluoroacetate salts (ref. H-2956 and H-7910, respectively). The Aβ(12-28) peptide was also synthesized by microwave solid-phase peptide synthesis (MW-SPPS) using Fmoc chemistry using the corresponding Fmoc protected amino acids. Cleavage from resin was performed using TFA/H_20/TIS (95:2,5:2,5) (V:V:V) and the peptide was precipitated with tert-butyl methyl ether. The peptide was purified by RP-HPLC using a VersaFlash® system and characterized by analytical RP-HPLC and MALDI-TOF-MS and compared to the commercial sample acquired from Bachem (H-7910).

Synthesis of Abeta (12-28)

H-VHHQKLVFFAEDVGSNK-OH

H-Val-His-His-Gln-Lys-Leu-Val-Phe-Phe-Ala-Glu-Asp-Val-Gly-Ser-Asn-Lys-OH

The peptide was synthesized both by conventional SPPS and by microwave MW-SPPS conditions.

General procedure for conventional manual Solid-Phase Peptide Synthesis (SPPS). Amino acids, building blocks, coupling reagents and prederivatized Fmoc-Lys(Boc)-Wang resin (0.7 mmol/g) were purchased from Novabiochem AG. All reagents used for synthesis were from analytical grade.

The peptide was synthesized manually following standard solid phase methods and Fmoc protocols on Fmoc-Lys(Boc)-Wang prederivatized resin using amino acids with orthogonal protections on lateral chains. Amide couplings were performed manually in a peptide synthesis column using DIC/HOBt in DMF under reciprocal oscillating agitation. Coupling efficiencies were monitored by Kaiser ninhydrin test. Fmoc groups were removed with a 20% piperidine in DMF solution.

Peptides were cleaved from the resin by shaking with a cleavage cocktail consisting of TFA:H_2O:TIS (95:2.5:2.5) for 2 h. The filtrate was evaporated, washed several times with ice-cold *tert*-butyl methyl ether and concentrated under reduced pressure. The crude peptide was precipitated with ice-cold *tert*-butyl methyl ether, filtered, redissolved in water and lyophilized. Crude peptide was purified by C-18 RP-HPLC (VersaFlash™ Flash Chromatography system) using a water-acetonitrile gradient and followed by lyophilization. The final pure peptide was characterized by MALDI-ToF MS and UPLC-ToF MS. Analytical RP-HPLC were performed using the following solvents A (0.1% TFA in H_2O) and B (0.1% TFA in acetonitrile) and the Nucleosil 100 RP-18 (5µm) C18 column (4x 250 mm). The retention time was compared to a commercially available sample from Novabiochem.

General procedure for Microwave Solid Phase Peptide Synthesis (MW-SPPS).

We followed similar procedures as describe in the literature:

> B. Bacsa S. Bosze C. O. Kappe *Direct solid-phase synthesis of the beta-amyloid (1-42) peptide using controlled microwave heating*. *J. Org. Chem.* **2010**, *75*, 2103-2106.

Equipment: CEM Liberty Blue system on a 0.1 mmol scale using Fmoc-Lys(Boc)Wang resin (0.7 mmol/g) and a 5-fold excess of reagents [0.2 M amino acid solution (in DMF) with 0.5 M DIC (in DMF) and 1.0 M Oxyma (in DMF) or 0.45 M HBTU (in DMF) and 2.0 M DIEA (in NMP with 10 fold excess)].

Using CEM for the synthesis of Abeta (12-28) two coupling procedures were used:

a) The “single coupling” procedure for all amino acids except Histidines at 75ºC; and

b) the “Double 50 c coupling” was used for Histidine. The sensitive FmocHis(Trt)-OH residues were built to into the sequence switching from 75ºC to room temperature in order to minimize racemization using an extended reaction time of 60 min and applying a double coupling strategy.

Single coupling

1. **Deprotection** :
    - Método microondas: **Standard deprotection**

T (ºC)	P (W)	Hold time (s)	Delta T (ºC)
70	155	15	2
90	30	50	1

    - Deprotection volumen: 4mL

2. **Wash**
    - Volume: 3mL
    - Drain time: 7
3. **Wash**
    - Volume: 3mL
    - Drain time: 7
4. **Wash**
    - Volume: 3mL
    - Drain time: 7
5. **Coupling:**
    - Reaction method: **Standard coupling**

T (ºC)	P (W)	Hold time (s)	Delta T (ºC)
75	170	15	2
90	30	110	1

    - Amino acid volumen: 2,5 mL
    - Activator volumen: 1 mL
    - Activator base volumen: 0,5 mL
    - Manifold wash volumen: 2mL

6. **Wash**
    - Volume: 3mL
    - Drain time: 7

Double 50c coupling

1. **Deprotection** :
    - Método microondas: **Standard deprotection**

T (ºC)	P (W)	Hold time (s)	Delta T (ºC)
70	155	15	2
90	30	50	1

    - Deprotection volumen: 4mL

2. **Wash**
    - Volume: 3mL
    - Drain time: 7
3. **Wash**
    - Volume: 3mL
    - Drain time: 7
4. **Wash**
    - Volume: 3mL
    - Drain time: 7
5. **Coupling:**
    - Reaction method: **50c coupling 8 min**

T (ºC)	P (W)	Hold time (s)	Delta T (ºC)
25	0	240	2
50	35	480	1

    - Amino acid volumen: 2,5 mL
    - Activator volumen: 1 mL
    - Activator base volumen: 0,5 mL
    - Manifold wash volumen: 2mL

6. **Wash**
    - Volume: 3mL
    - Drain time: 7

7. **Coupling**
    - Reaction method: **50c coupling 8 min**

T (ºC)	P (W)	Hold time (s)	Delta T (ºC)
25	0	240	2
50	35	480	1

    - Amino acid volumen: 2,5 mL
    - Activator volumen: 1 mL
    - Activator base volumen: 0,5 mL
    - Manifold wash volumen: 2mL

8. **Wash**
    - Volume: 3
    - Draint time: 7

Common steps to all the couplings:

Final deprotection

1. **Deprotection** :
   - Método microondas: **75º Initial deprotection**

T (ºC)	P (W)	Hold time (s)	Delta T (ºC)
75	100	30	2

   - Deprotection volumen: 3mL

2. **Deprotection:**
   - Método microondas: **75º deprotection**

T (ºC)	P (W)	Hold time (s)	Delta T (ºC)
75	100	180	2

   - Deprotection volumen: 3mL

3. **Wash**
   - Volume: 2mL
   - Drain time:5
4. **Wash**
   - Volume: 2 mL
   - Drain time:5
5. **Wash**
   - Volume: 3mL
   - Drain time: 5

Resin swelling

- Volume: 10
- Time: 300

Characterization of Abeta (12-28): HPLC and MS.

HPLC analysis

Analytical RP-HPLC with a Nucleosil 100 RP-18 (5µm) C18 column (4x 250 mm). Flow rate: 1mL/min. Solvents used: A: 0.1% TFA in H_2O; B: 0.1% TFA in acetonitrile

Gradient: From A:B (80:20) to A:B (20:80) in 25 min.
RT (BACHEM SAMPLE, REF 4014778) = 9.19 min

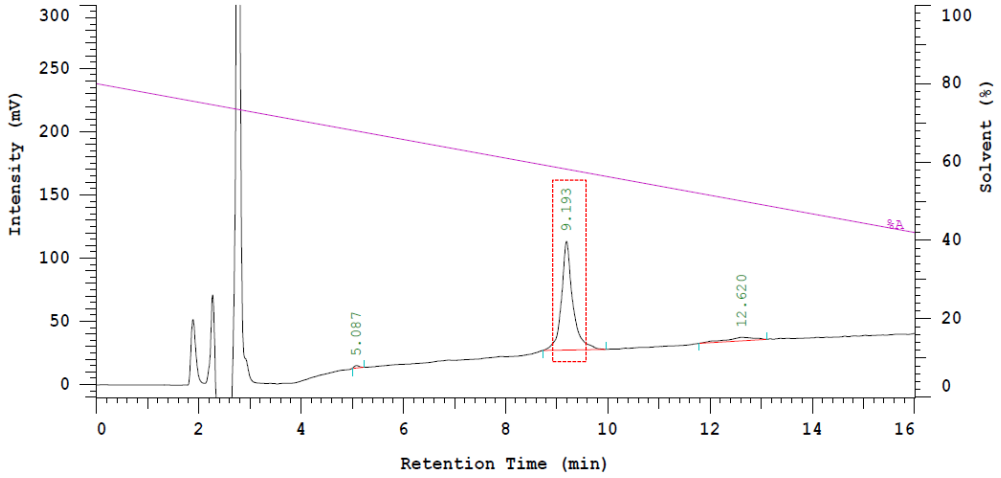

Figure S11: Analytical HPLC of Abeta(12-28) from Bachem.

After VersaFlash™ RP-HPLC purification

From A:B (80:20) to A:B (20:80) in 25 min. RT = 9.1 min

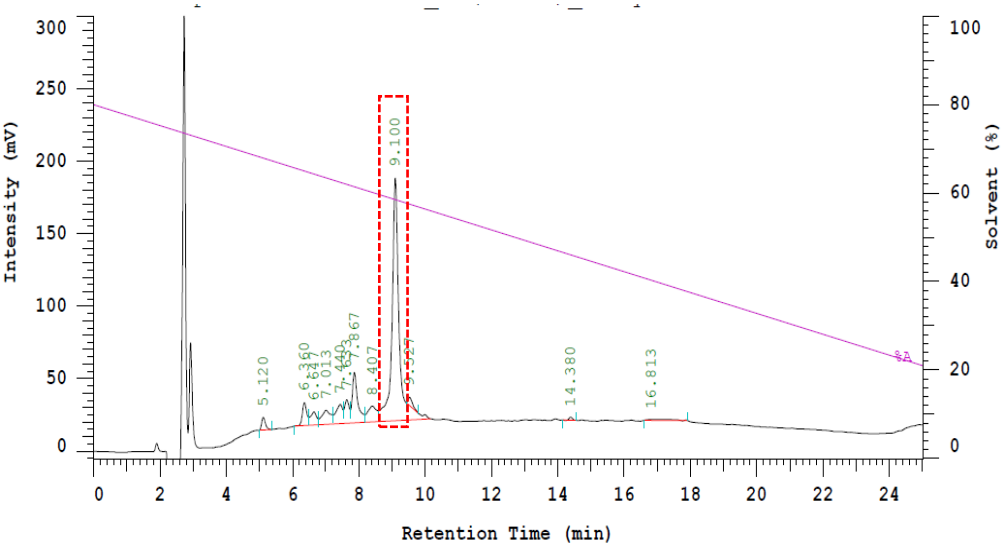

Figure S12: HPLC of purified Abeta(12-28) obtained by SPPS.

UPLC-ToF MS

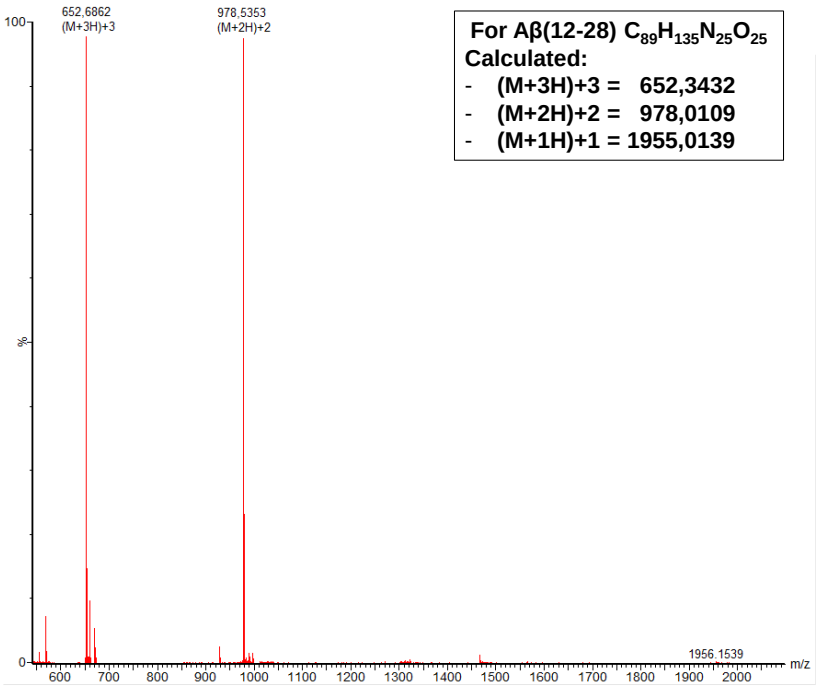

Figure S13: UPLC-ToF-MS of Abeta(12-28) obtained by SPPS.

Isothermal Titration Calorimetry (ITC) studies: thermodynamic parameters for the Aβ(12-28)/TTR/DCPA interaction

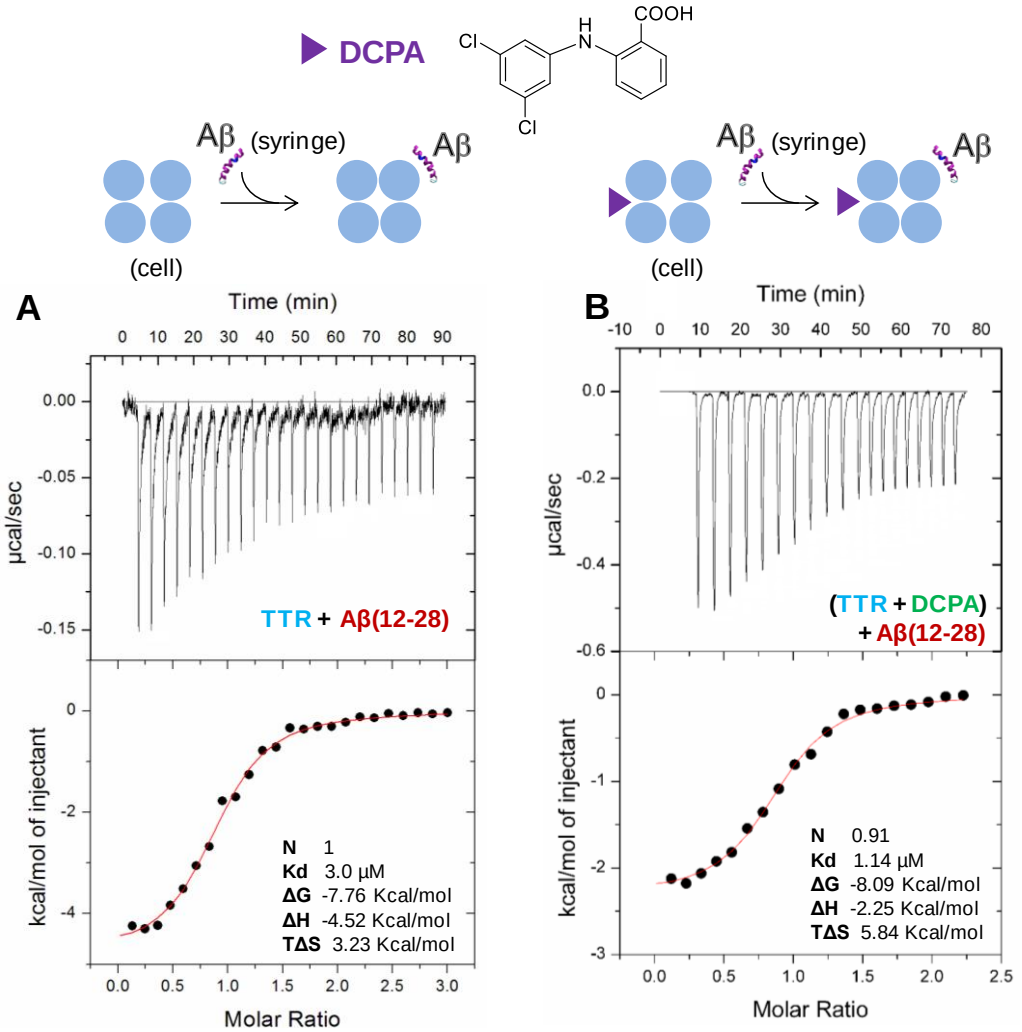

Figure S14: ITC analysis of the interactions: A) the binary complex TTR + Aβ(12-28); B) the ternary complex of [TTR + DCPA)] and Aβ(12-28). All these ITC studies were performed at pH 7.4 in 25 mM HEPES buffer, 10 mM glycine and 5% DMSO (final concentration) at 25 ºC.

Table S6: Thermodynamic parameters for the Aβ(12-28) / TTR interaction and the ternary interaction (TTR + DCPA) + Aβ(12-28) .

Assay	n	K_d (µM)	ΔH (Kcal/mol)	TΔS (Kcal/mol)	ΔG (Kcal/mol)
TTR + Aβ(12-28)	1	3,1	-4,52	3,23	-7,76
(TTR + DCPA) + Aβ(12-28)	1	1,1	-2,25	5,84	-8,09

Isothermal Titration Calorimetry (ITC) studies: thermodynamic parameters for the Aβ(12-28)/TTR/DFPA interaction

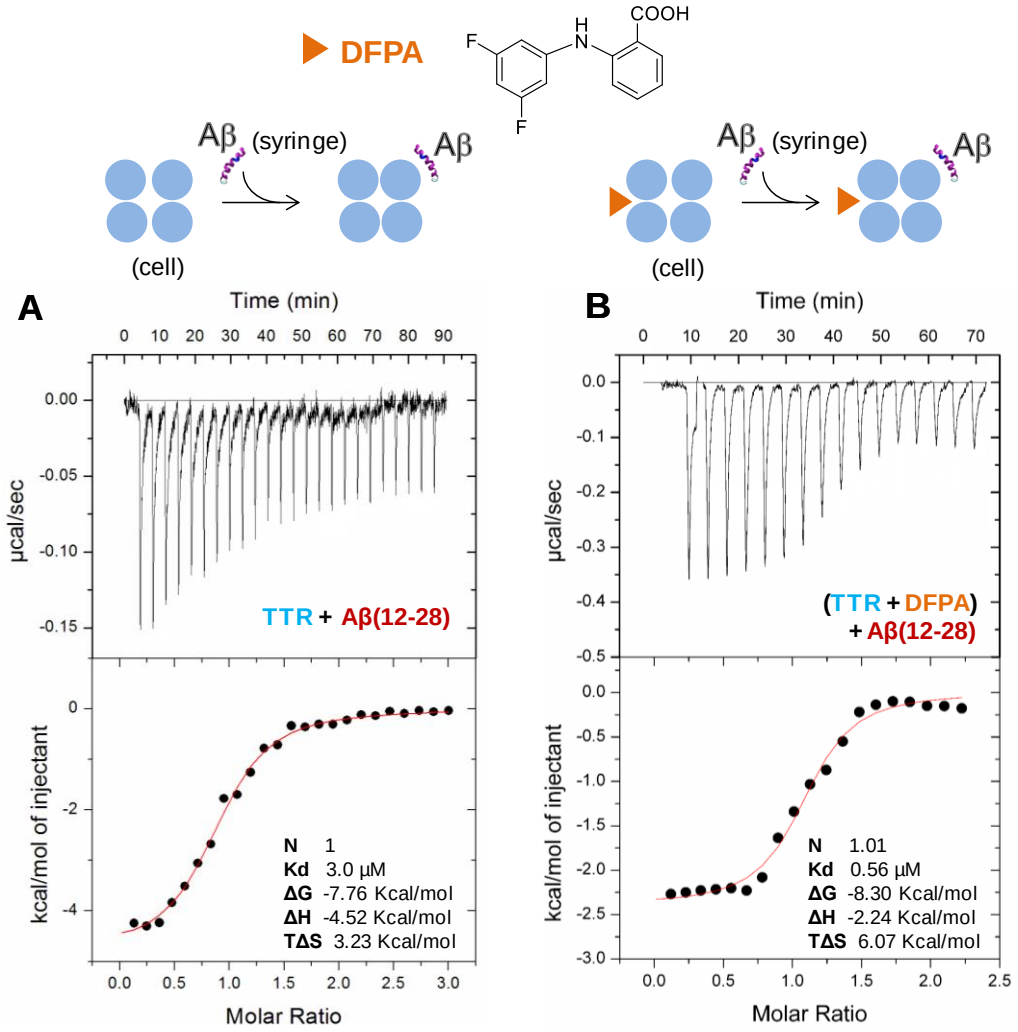

Figure S15: ITC analysis of the interactions: A) the binary complex TTR + Aβ(12-28); B) the ternary complex of [TTR + DFPA)] and Aβ(12-28). All these ITC studies were performed at pH 7.4 in 25 mM HEPES buffer, 10 mM glycine and 5% DMSO (final concentration) at 25 ºC.

Table S7: Thermodynamic parameters for the Aβ(12-28) / TTR interaction and the ternary interaction (TTR + DFPA) + Aβ(12-28).

Assay	n	K_d (µM)	ΔH (Kcal/mol)	TΔS (Kcal/mol)	ΔG (Kcal/mol)
TTR + Aβ(12-28)	1	3,1	-4,52	3,23	-7,76
(TTR + DFPA) + Aβ(12-28)	1	0,6	-2,24	6,07	-8,30

Preliminary data for additional compounds using the HTS system:

Triiodophenol, Epigallocatechin gallate (EGCG), Resveratrol (RESV) and the repurposed drug tolcapone.

Triodophenol

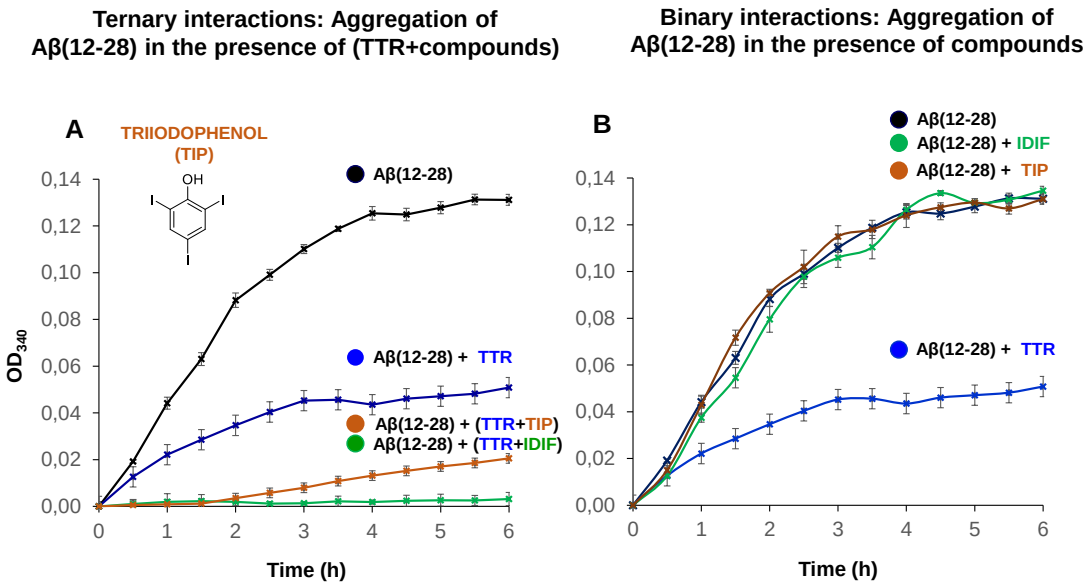

Figure S16. Aggregation kinetics of Aβ(12-28) measured by the turbidity assay at 37 °C over 6 h. A) Aggregation of Aβ(12-28): in the presence of TTR (binary complex) and in the presence of TTR + IDIF (ternary complex) and in the presence of TTR + TIP (ternary complex) . Studies were performed at pH 7.4 in 25 mM HEPES buffer, 10 mM glycine and 5% DMSO (final concentration) at 37 ºC. B) Aggregation kinetics of Aβ(12-28) measured by the turbidity assay at 37 °C over 6 h in the presence of TTR, in the presence of IDIF and in the presence of TIP.

Miroy GJ, Lai Z, Lashuel HA, Peterson SA, Strang C, Kelly JW. Inhibiting transthyretin amyloid fibril formation via protein stabilization. *Proc Natl Acad Sci U S A.* **1996**, 93(26):15051-6. doi: 10.1073/pnas.93.26.15051.

Dolado, I.; Nieto, J.; Saraiva, M. J. M.; Arsequell, G.; Valencia, G.; Planas, A. Kinetic assay for high-throughput screening of in vitro transthyretin amyloid fibrillogenesis inhibitors. *J. Comb. Chem.* **2005**, 7, 246−252.

Resveratrol (RESV) (3,5,4′-trihydroxy-trans-stilbene)

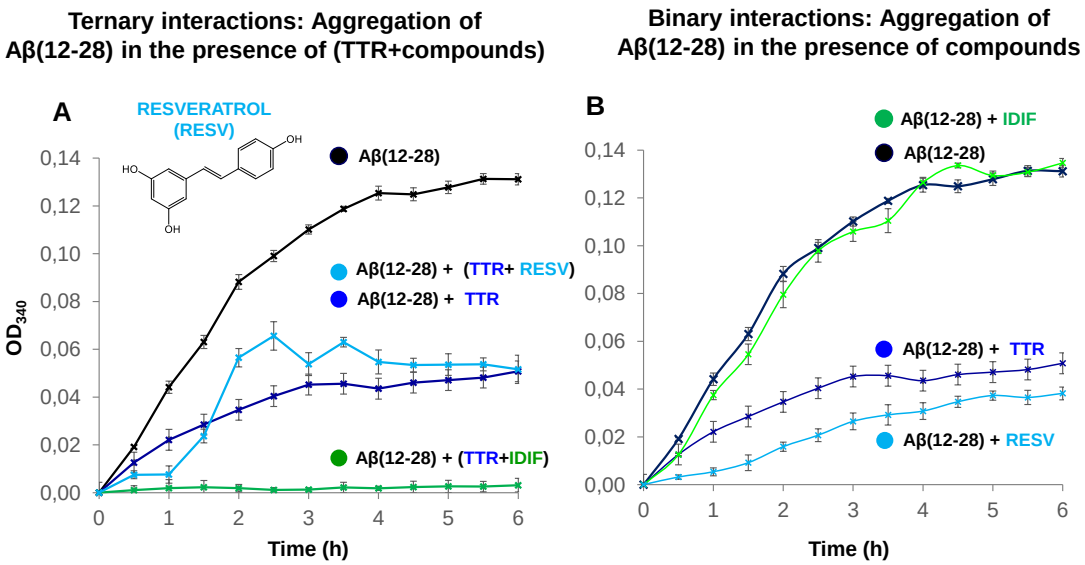

Figure S17. Aggregation kinetics of Aβ(12-28) measured by the turbidity assay at 37 °C over 6 h. A) Aggregation of Aβ(12-28): in the presence of TTR (binary complex) and in the presence of TTR + IDIF (ternary complex) and in the presence of TTR + RESV (ternary complex) . Studies were performed at pH 7.4 in 25 mM HEPES buffer, 10 mM glycine and 5% DMSO (final concentration) at 37 ºC. B) Aggregation kinetics of Aβ(12-28) measured by the turbidity assay at 37 °C over 6 h in the presence of TTR, in the presence of IDIF and in the presence of RESV.

Klabunde T, Petrassi HM, Oza VB, Raman P, Kelly JW, Sacchettini JC. Rational design of potent human transthyretin amyloid disease inhibitors [published correction appears in Nat Struct Biol 2000 May;7(5):431]. *Nat Struct Biol.* **2000**, 7312-321. doi:10.1038/74082.

Ladiwala AR, Lin JC, Bale SS, Marcelino-Cruz AM, Bhattacharya M, Dordick JS, Tessier PM. Resveratrol selectively remodels soluble oligomers and fibrils of amyloid Abeta into off-pathway conformers. *J Biol Chem.* **2010**, 285, 24228-24237. doi:10.1074/jbc.M110.133108

Epigallocatechin gallate (EGCG)

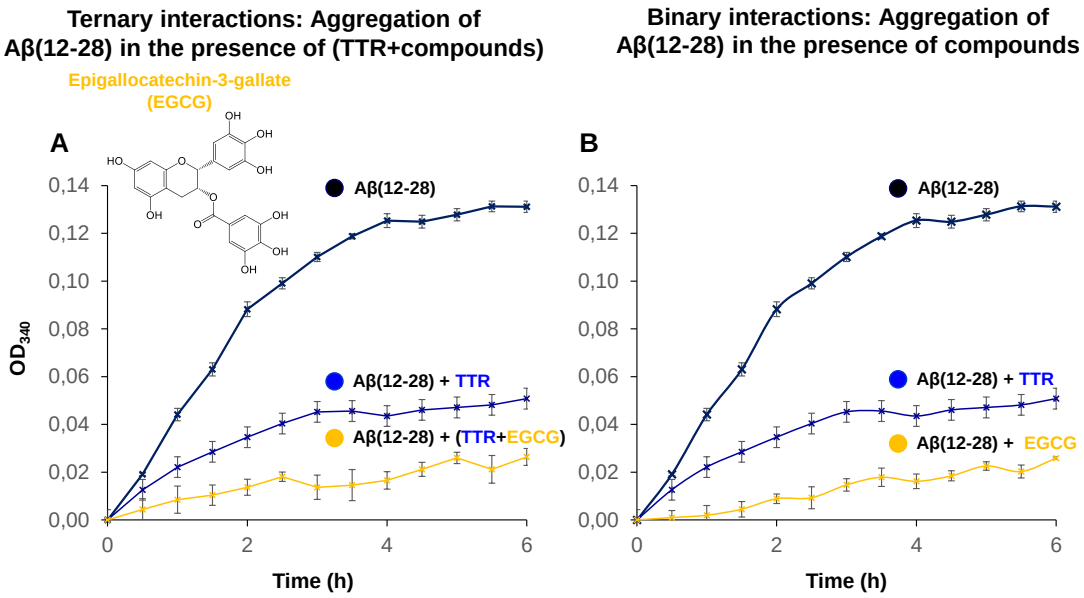

Figure S18. Aggregation kinetics of Aβ(12-28) measured by the turbidity assay at 37 °C over 6 h. A) Aggregation of Aβ(12-28): in the presence of TTR (binary complex) and in the presence of TTR + IDIF (ternary complex) and in the presence of TTR + EGCG (ternary complex) . Studies were performed at pH 7.4 in 25 mM HEPES buffer, 10 mM glycine and 5% DMSO (final concentration) at 37 ºC. B) Aggregation kinetics of Aβ(12-28) measured by the turbidity assay at 37 °C over 6 h in the presence of TTR, in the presence of IDIF and in the presence of EGCG.

Miyata M., Sato T., Kugimiya M., Sho M., Nakamura T., Ikemizu S., Chirifu M., Mizuguchi M., Nabeshima Y., Suwa Y., et al. The crystal structure of the green tea polyphenol (-)-epigallocatechin gallate-transthyretin complex reveals a novel binding site distinct from the thyroxine binding site. *Biochemistry*. **2010**; *49*, 6104–6114. doi: 10.1021/bi1004409.

Ferreira N, Saraiva MJ, Almeida MR. Natural polyphenols inhibit different steps of the process of transthyretin (TTR) amyloid fibril formation. *FEBS Lett.* **2011**, 585, 2424-30.

Gimeno, A., Santos, L.M.; Alemi, M.; Rivas, J.; Blasi, D.; Cotrina, E.Y.; Llop, J.; Valencia, G.; Cardoso, I.; Quintana, J.; Arsequell, G.; Jiménez-Barbero, J. Insights on the Interaction between Transthyretin and Aβ in Solution. A Saturation Transfer Difference (STD) NMR Analysis of the Role of Iododiflunisal. *J. Med. Chem.* **2017**, 60, 5749-5758. doi:10.1021/acs.jmedchem.7b00428.

Tolcapone

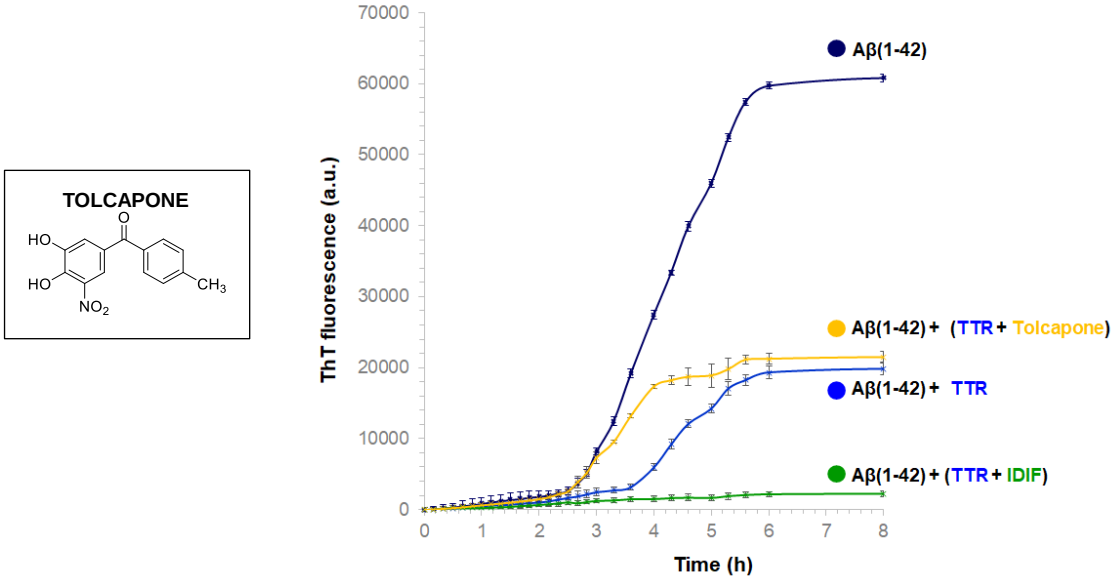

Figure S19: ThT assays of the aggregation of Aβ(1-42) alone (20 μM), in complex with TTR (10 μM), or in complex with TTR stabilized with different small compounds (20 μM) (TTR/Tolcapone, and TTR/Tafamidis). ThT fluorescence was measured at 37 ºC each 10 min for 3h, then each 20 min from 3 h to 6 h, and then at 8 h. Samples were assayed in duplicate and are representative of three different replicates (n=6). Negative controls (buffer solutions) are not shown.

The following ITC study on the repurposed drug tolcapone is included at the Supporting Information in a recent paper that will be published in *Journal of Alzheimer's Disease (JAD).* (https://www.j-alz.com/vol77-1): **Oral Treatment with Iododiflunisal Delays Hippocampal Amyloid-β Formation in a Transgenic Mouse Model of Alzheimer's Disease: A Longitudinal in vivo Molecular Imaging Study.** Luka Rejc, Vanessa Gómez-Vallejo, Xabier Rios, Unai Cossío, Zuriñe Baz, Edurne Mujica, Tiago Gião, Ellen Y. Cotrina, Jesús Jiménez-Barbero, Jordi Quintana, Gemma Arsequell, Isabel Cardoso, Jordi Llop. *J. Alzheimer's Disease* (2020). (In press).

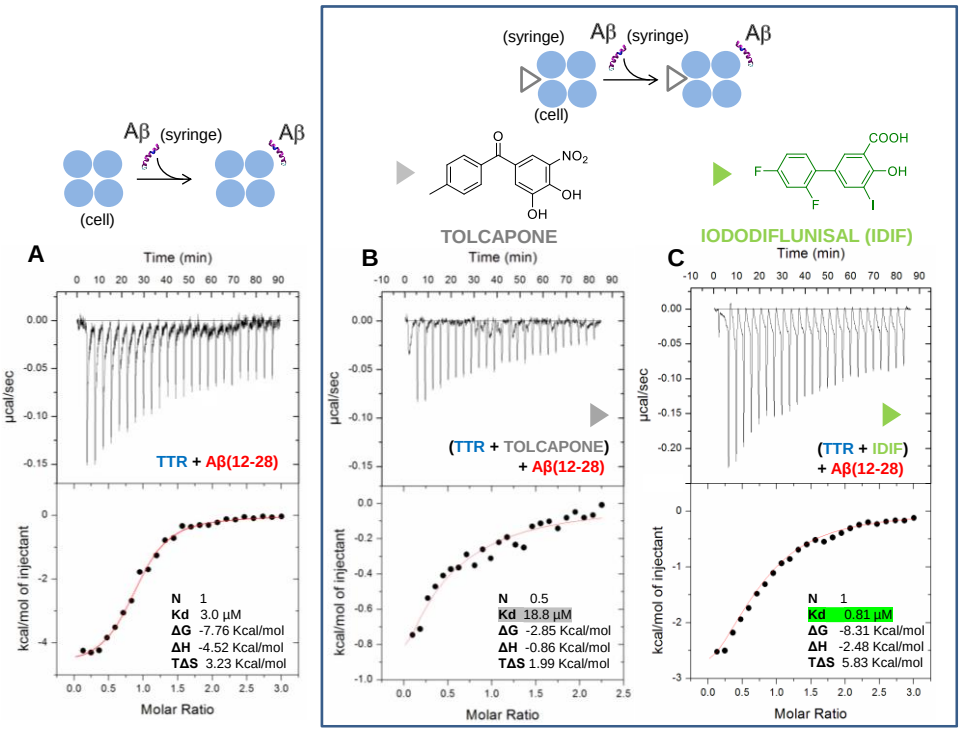

Figure S20: ITC analysis of the interactions: A) the binary complex TTR + Aβ(12-28); B) the ternary complex of [TTR + TOLCAPONE)] and Aβ(12-28); and C) the ternary complex of [TTR + IDIF)] and Aβ(12-28).. All these ITC studies were performed at pH 7.4 in 25 mM HEPES buffer, 10 mM glycine and 5% DMSO (final concentration) at 25 ºC.